PHYSICAL REVIEW D **95,** 055014 (2017)

Anarchy with hierarchy: A probabilistic appraisal

K. S. Babu,[*] Alexander Khanov,[†] and Shaikh Saad[‡]

Department of Physics, Oklahoma State University, Stillwater, Oklahoma 74078, USA

(Received 6 January 2017; published 16 March 2017)

The masses of the charged fermion and the mixing angles among quarks are observed to be strongly hierarchical, while analogous parameters in the neutrino sector appear to be structureless or anarchical. We develop a class of unified models based on $SU(5)$ symmetry that explains these differing features probabilistically. With the aid of three input parameters that are hierarchical, and with the assumption that all the Yukawa couplings are uncorrelated random variables described by Gaussian distributions, we show by Monte Carlo simulations that the observed features of the entire fermion spectrum can be nicely reproduced. We extend our analysis to an $SU(5)$-based flavor $U(1)$ model making use of the Froggatt-Nielsen mechanism where the order one Yukawa couplings are modeled as random variables, which also shows good agreement with observations.

DOI: 10.1103/PhysRevD.95.055014

I. INTRODUCTION

Although the Standard Model (SM) of particle physics has been highly successful, it does not address some of the observed phenomena. For example, neutrinos in the SM are strictly massless. Nonzero masses for the neutrinos have been firmly established through oscillations experiments conducted with atmospheric [1], solar [2], accelerator [3], and reactor [4] neutrinos, requiring modification of the minimal model. An aesthetic shortcoming of the SM, arising from the enormous freedom available in the Yukawa Lagrangian, is that it provides very little insight into the masses and mixings of quarks and leptons. This shortcoming is often dubbed the "flavor puzzle" and many extensions of the SM are constructed to address this issue. The purpose of this paper is to interpret the apparently diverse set of flavor parameters—quark masses, quark mixing angles, charged fermion masses, neutrino masses, and leptonic mixing angles—in a unified fashion probabilistically.

The observed masses in the charged fermion sector show a hierarchical structure, with the strongest hierarchy seen in the up-type quark sector, and a somewhat milder hierarchy seen in the down-type quark and charged lepton sectors. These mass parameters, at the momentum scale $\mu = \mathrm{M_Z}$, are approximately given by (in units of $m_t = 1$)

$$\begin{aligned} &m_u \sim 7.5 \times 10^{-6}; \quad m_c \sim 3.6 \times 10^{-3}; \quad m_t \sim 1; \\ &m_d \sim 1.6 \times 10^{-5}; \quad m_s \sim 3 \times 10^{-4}; \quad m_b \sim 1.6 \times 10^{-2}; \\ &m_e \sim 3 \times 10^{-6}; \quad m_\mu \sim 6 \times 10^{-4}; \quad m_\tau \sim 1 \times 10^{-2}. \end{aligned} \tag{1.1}$$

In contrast, the two neutrino squared-mass differences measured in oscillation experiments yield values given by [5]

$$\Delta m^2_{\mathrm{sol}} \sim 7.5 \times 10^{-5}\ \mathrm{eV}^2 \quad \text{and} \quad \Delta m^2_{\mathrm{atm}} \sim 2.5 \times 10^{-3}\ \mathrm{eV}^2. \tag{1.2}$$

Adopting a normal ordering of the mass spectrum with $m_1 < m_2 \ll m_3$ with m_i being the neutrino masses, these values would indicate a mild or almost no hierarchy with $m_2/m_3 \sim 1/5$, quite different from the hierarchy seen in the other sectors [cf. Eq. (1.1)]. Additionally, the intergenerational mixing angles in the quark sector are found to be small, while the leptonic mixing angles are measured to be large,

$$\begin{aligned} &\theta_{12}^{\mathrm{CKM}} \sim 13^\circ; \quad \theta_{23}^{\mathrm{CKM}} \sim 2.4^\circ; \quad \theta_{13}^{\mathrm{CKM}} \sim 0.2^\circ; \\ &\theta_{12}^{\mathrm{PMNS}} \sim 34^\circ; \quad \theta_{23}^{\mathrm{PMNS}} \sim 38^\circ; \quad \theta_{13}^{\mathrm{PMNS}} \sim 9^\circ. \end{aligned} \tag{1.3}$$

Understanding these patterns observed in the fermion spectrum is a fundamental unresolved problem in particle physics. Various attempts have been made to explain the hierarchy in the charged fermion masses and mixings, adopting highly regulated mass matrices supported by flavor symmetries (for a review see Ref. [6]). On the other hand, random structureless matrices may be better suited to explain the nonhierarchical mass spectrum and the large mixing angles observed in the neutrino sector [7]. The use of such random matrices to explain neutrino mixing angles has been termed "anarchy hypothesis." A probability measure should be specified for these random matrices such that the matrix elements remain random after a basis transformation. For random unitary matrices this is achieved uniquely by the Haar measure [8]. Such matrices have been shown to be successful in explaining the observed large mixing angles in the neutrino sector

[*]babu@okstate.edu
[†]khanov@okstate.edu
[‡]shaikh.saad@okstate.edu

[7–14]. When basis independence of the random matrix is combined with the requirement that each entry of the matrix has a distribution independent of other entries, the measure gets determined uniquely to be Gaussian [15–18]. Anarchical neutrino mixing angles as well as mass ratios have been analyzed with the Gaussian measure in Ref. [18].

In this paper we unify the anarchy hypothesis in the neutrino sector with the hierarchy observed in the quark and charged lepton sectors [8,19–21], and we analyze the resulting models from a probabilistic perspective. Such a unification is achieved in the framework of $SU(5)$ grand unified theories, which treat quarks and leptons on similar footing. For concreteness we adopt a supersymmetric framework, which admits a one step symmetry breaking of $SU(5)$ down to the minimal supersymmetric standard model (MSSM). These models have at most three parameters which are hierarchical and determined from a fit to data. They also contain five complex Yukawa coupling matrices which are taken to be structureless or anarchical. Elements of these Yukawa coupling matrices are treated as uncorrelated random variables obeying Gaussian distributions. We perform Monte Carlo simulations of this framework and compare theoretical expectations with experimental data, which show good agreement.

Our main analysis is focused on the Yukawa coupling structure obtained in supersymmetry (SUSY) $SU(5)$ unified theories where the three families of 10_i fermions mix with vectorlike fermions belonging to $10_\alpha + \overline{10}_\alpha$ representations that have grand unified theory (GUT) scale masses [19]. A variant of this model using the Froggatt-Nielsen mechanism [22], where the three families of 10_i fermions are distinguished by a flavor $U(1)$ symmetry while the three families of $\bar{5}_i$ are universal, is also analyzed allowing for effective nonrenormalizable operators [8]. This class of models is a special case of the general class, with only two hierarchical input parameters. A second variant, also using a similar $U(1)$ flavor symmetry, which now distinguishes the first family $\bar{5}_1$ from the $\bar{5}_{2,3}$ fields is also analyzed, with a single hierarchy parameter as input [23,24]. Good fit to the entire fermion spectrum is obtained in all cases with the Yukawa couplings taking on uncorrelated Gaussian distributions.

It should be noted that ways to understand the neutrino mass anarchy along with the charged fermion mass hierarchy have been explored in extra dimensional models with some success [25–28]. These models have not yet been subject to a detailed Monte Carlo analysis for testing quantitatively the goodness of the fit. The (renormalizable) models we discuss here share some common qualitative features with these extra dimensional models.

We also develop a constrained Monte Carlo simulation method to evaluate the figure of merit of the uncorrelated Gaussian distributions adopted for the random variables. In this method we calculate a specific projection of the probability density distribution of the original random parameters onto a surface that corresponds to random parameters that satisfy the experimental constraints. The figure of merit that is optimized in this simulation is the distortion of the distributions of the random parameters with respect to their original (unconstrained) distributions. This constrained Monte Carlo result can be thought of as a multidimensional analog of the Kolmogorov-Smirnov statistical test for a single variable. Our analysis shows that the distortions from the original Gaussian distributions are not much, suggesting a good quality fit.

While the class of models studied here cannot be tested in their precise predictions, they may become strongly favored or disfavored once we know more about the neutrino mass and mixing parameters. With an anarchical structure the CP-violating parameter $\sin\delta$ in the neutrino sector is found to be peaked at maximal values (± 1), although variations from these peak values are not excluded. The probability distribution of the neutrino mass ratio m_1/m_2 is peaked around 0.3, with the probability of measuring it below $1/100$ found to be about 4%.

This paper is organized as follows. In Sec. II we present our unified SUSY $SU(5)$ model which allows for the mixing of the three families of 10_i with vectorlike fermions in the $10_\alpha + \overline{10}_\alpha$ representations. Here we also present special cases of this general framework making use of flavor $U(1)$ symmetries. In Sec. III we present the results of our Monte Carlo simulations for the fermion mass and mixing parameters for the main model as well as for its variants. In Sec. IV we develop a new constrained Monte Carlo method to evaluate the goodness of the fits and compare the distortions of these new distributions from the original Gaussian distributions. In Sec. V we conclude. Two Appendixes contain further details of our analysis. In Appendix A we present the distributions of the various flavor observables for the special cases with flavor $U(1)$ symmetries with either two or one parameter(s). In Appendix B we present the distributions of the flavor observables obtained from our constrained Monte Carlo simulation for the main model.

II. UNIFYING ANARCHY WITH HIERARCHY IN $SU(5)$

As noted in the Introduction, grand unified theories based on $SU(5)$ allow for a unified description of anarchy in the neutrino sector and hierarchy in the quark sector. We work in the context of SUSY $SU(5)$. The GUT symmetry spontaneously breaks down to the MSSM at an energy scale of 2×10^{16} GeV. The effective low energy theory is the MSSM. Our focus is the Yukawa couplings of the quarks and leptons in these theories. At the MSSM level, the Yukawa coupling matrices for the up quarks, down quarks, charged leptons, Dirac neutrinos, and the right-handed Majorana neutrinos derived from these models will take the form [19]

$$Y_U = H^T Y_U^0 H, \tag{2.1}$$

$$Y_D = \epsilon_4 Y_D^0 H, \tag{2.2}$$

$$Y_L = \epsilon_4 H^T Y_L^0, \tag{2.3}$$

$$Y_N = Y_N^0, \tag{2.4}$$

$$Y_R = Y_R^0. \tag{2.5}$$

Here the superpotential couplings are written as $(f_i^c (Y_f)_{ij} f_j) H_f$ with H_u and H_d denoting the two Higgs fields of MSSM. The fermion mass matrices obtained from Eqs. (2.1)–(2.5) have the form

$$M_U = Y_U v_u, \quad M_D = Y_D v_d, \quad M_L = Y_L v_d, \quad \text{and}$$
$$M_N = Y_N v_u, \quad M_R = Y_R v_R \tag{2.6}$$

with v_u and v_d being the vacuum expectation values of H_u and H_d. We have assumed the right-handed Majorana neutrino masses arise through the vacuum expectation value (VEV) v_R of a SM singlet field. In $SU(5)$ unified theories, bare Majorana masses for the gauge singlet right-handed neutrinos may be written down. If such bare masses are adopted, the scale v_R should be treated as an overall scale in the Majorana mass matrix. The light neutrino mass matrix, obtained via the seesaw mechanism [29], has the form

$$M_\nu = (Y_N^T Y_R^{-1} Y_N) \frac{v_u^2}{v_R}. \tag{2.7}$$

An explicit derivation of the Yukawa matrices of Eqs. (2.1)–(2.5) based on $SU(5)$ will be given in the next subsection. Here we note their salient features which enable the unification of hierarchy and anarchy.

The matrix H in Eqs. (2.1)–(2.3) is Hermitian, which may be chosen to be diagonal, real, and positive,

$$H = \mathrm{diag}(\epsilon_1, \epsilon_2, \epsilon_3). \tag{2.8}$$

Here $\epsilon_1 \ll \epsilon_2 \ll \epsilon_3 \sim 1$ are input parameters of the model which take hierarchical values [19]. $\epsilon_3 = 1$ can be chosen by redefining other parameters of the model. These parameters arise in the model by virtue of mixing between the three chiral 10_i-plets of fermions with vectorlike $10_\alpha + \overline{10}_\alpha$ of fermions with GUT scale masses. Y_f^0 in Eqs. (2.1)–(2.5) are the "bare" Yukawa coupling matrices—coupling matrices in the absence of mixing with the vectorlike $10_\alpha + \overline{10}_\alpha$ fermions—which will be assumed to have no specific structure. $SU(5)$ invariance implies that the same H multiplies all the bare Yukawa coupling matrices in Eqs. (2.1)–(2.3). Note that H appears on the right of Y_D^0, while it appears on the left of Y_L^0. This occurs in $SU(5)$ since the d^c field—the $SU(2)_L$ singlet down-type antiquark—is unified with the left-handed lepton doublet in a $\bar{5}$ representation. As a consequence, the left-handed lepton mixing angles will be of order unity, simultaneously with order one mixing in the right-handed down quark sector (which are unobservable). Note also that the mass matrices for down quarks and charged leptons are "lop-sided" [19,30–33]. Furthermore, H appears on both sides of Y_U^0 in Eq. (2.1) [while it appears on only one side of Y_D^0 and Y_E^0 in Eqs. (2.2) and (2.3)], which is due to the presence of u and u^c fields in the same 10-plet of $SU(5)$. As a result, the mass hierarchy in the up-quark sector would be stronger compared to the hierarchy in the down-quark and charged lepton sectors,

$$m_d : m_s : m_b \sim \epsilon_1 : \epsilon_2 : 1, \tag{2.9}$$

$$m_e : m_\mu : m_\tau \sim \epsilon_1 : \epsilon_2 : 1, \tag{2.10}$$

$$m_u : m_c : m_t \sim \epsilon_1^2 : \epsilon_2^2 : 1. \tag{2.11}$$

Such a pattern is consistent with observations.

As for the mixing angles, Eqs. (2.1)–(2.5) will lead to

$$V_{ij}^{\mathrm{CKM}} \sim \frac{\epsilon_i}{\epsilon_j}, \qquad i < j;$$
$$V_{ij}^{\mathrm{lepton}} \sim 1, \qquad i < j. \tag{2.12}$$

That is, small quark mixings are realized along with large leptonic mixings in these models.

The parameter ϵ_4 in Eqs. (2.2) and (2.3) is a third hierarchy parameter, corresponding to an overall suppression of Y_D and Y_L compared to Y_U, which has its origin in the mixing of Higgs doublets at the GUT scale. (In certain minimal models such mixings may be absent, in which case $\epsilon_4 = 1$. We have investigated this scenario and found that the goodness of the fit to data is poor.) Since there is no hierarchy parameter in Y_N and Y_R in Eqs. (2.4) and (2.5), the light neutrino masses do not exhibit any hierarchy in this construction [see Eq. (2.7)].

The form of the Yukawa matrices given in Eqs. (2.1)–(2.5) may also be obtained in other ways in the context of $SU(5)$ unification. It has been suggested that these forms may follow if the 10-plet fermions are composite, while the $\bar{5}$-plet fermions are elementary [20]. Alternatively, if there is a flavor symmetry that distinguishes the three families of 10-plets, with the $\bar{5}$-plets being indistinguishable by this symmetry [8], the forms of Eqs. (2.1)–(2.5) may follow with the restriction that $\epsilon_1 \simeq \epsilon_2^2$. A flavor-dependent $U(1)$ symmetry that distinguishes $\bar{5}_1$ from $\bar{5}_{2,3}$ can lead to yet another constrained model, which may have only a single hierarchy parameter [23,24]. We shall analyze these special cases as well.

A. Anarchy and hierarchy via mixing with vectorlike fermions

In this subsection we provide an explicit construction of the fermion Yukawa matrices of Eqs. (2.1)–(2.5) based on $SU(5)$ symmetry. The setup that we present here is quite general, and we will discuss some of its special cases in subsequent subsections. The construction involves mixing of the chiral families in the 10_i representations of $SU(5)$ with vectorlike $10_\alpha + \overline{10}_\alpha$ fermions which have GUT scale masses. Such mixings provide the needed hierarchy factors to explain the charged fermion masses and quark mixing angles. All the Yukawa couplings of the model will be assumed to be structureless or anarchical. This applies to the Yukawa couplings in the quark sector, the charged lepton sector, and the neutrino sector universally. Thus, in the spirit of anarchy, these Yukawa coupling matrix elements will all be taken as uncorrelated random variables with Gaussian distributions.

The three families of fermions belong to the $10_i + \bar{5}_i$ multiplets of $SU(5)$ ($i = 1$–3 is the generation index). Quarks and leptons are unified in these multiplets as $10_i = \{e_i^c, u_i^c, Q_i\}$ and $\bar{5}_i = \{L_i, d_i^c\}$, where $Q_i = (u_i d_i)^T$ and $L_i = (\nu_i e_i)^T$. To generate small neutrino masses via the seesaw mechanism three $SU(5)$ singlet fermions 1_i (ν_i^c) are introduced. If only a $5_H + \bar{5}_H$ Higgs pair is involved in the Yukawa couplings as usually assumed in minimal SUSY $SU(5)$, the relation $M_L = M_D^T$ will result among the down-type quark and charged lepton mass matrices, which is unacceptable. To correct for this at the renormalizable level, we extend the Higgs sector by introducing a $45_H + \overline{45}_H$ pair [34]. Then the Yukawa superpotential is given by (assuming the usual R-parity)

$$\mathcal{W}_Y = 10_i Y^5_{ij} 10_j 5_H + 10_i Y^{45}_{ij} 10_j 45_H + \bar{5}_i Y^{\bar{5}}_{ij} 10_j \bar{5}_H + \bar{5}_i Y^{\overline{45}}_{ij} 10_j \overline{45}_H + \bar{5}_i Y^1_{ij} 1_j 5_H + \frac{1}{2}(M_R)_{ij} 1_i 1_j, \tag{2.13}$$

where $Y^{\bar{5}}$, $Y^{\overline{45}}$, and Y^1 are general complex matrices, while Y^5 and Y^{45} are complex symmetric and antisymmetric matrices. These "bare" Yukawa coupling matrix elements (as well as the Majorana mass terms M_R for the right-handed neutrinos, up to an overall scale) will all be taken to be random variables obeying Gaussian distributions.

The model also contains a set of vectorlike fermions belonging to $10_\alpha + \overline{10}_\alpha$ representations, where $\alpha = 1, 2, \ldots, n$ where n is the number of copies used. The choice of $n = 3$ is natural, in which case there would be three pairs of such fields. The superpotential now admits additional mass terms given by

$$\mathcal{W}_Y \supset m_{\alpha j} \overline{10}_\alpha 10_j + M_{\alpha\beta} \overline{10}_\alpha 10_\beta, \tag{2.14}$$

where the first term represents the mixing of the ordinary fermions with the vectorlike fermions and the second term generates bare masses for these vectorlike fermions. Other possible gauge invariant couplings are assumed to be absent due to additional symmetries. An example of such a symmetry is a $Z_2 \times Z_2$ with the vectorlike fermions $\overline{10}_\alpha$ being odd under the first Z_2, and the rest of the fields being even. This choice will prevent unwanted terms of the type $\overline{10}_\alpha 10_\beta 24_H$ and $\overline{10}_\alpha 10_i 24_H$, involving the $SU(5)$ breaking Higgs field 24_H. Such a Z_2 is broken by the terms in Eq. (2.14), but only softly. Under the second Z_2, both 10_α and $\overline{10}_\alpha$ fields are odd, while the remaining fields are even. This Z_2, which is also broken softly by the first term in Eq. (2.14), will prevent mixed Yukawa coupling of the type $10_i 10_\alpha 5_H$. (This second Z_2 is optional, since the presence of mixed Yukawa couplings of the type $10_i 10_\alpha 5_H$ do not have any effect on our analysis).

In Eq. (2.14) the mass terms m and M are SM singlets and will be assumed to be of order the GUT scale. The presence of these terms in the Yukawa Lagrangian modifies the structure of the mass matrices of the SM fermions. From Eq. (2.14), the heavy states are found to be $10^H_\alpha \propto m_{\alpha i} 10_i + M_{\alpha\beta} 10_\beta$, with the light states 10^L_i being orthogonal to the 10^H_α states. This system can be inverted to express 10_i and 10_α in terms of $10^{L,H}$ states: $10_i = (H 10^L + H' 10^H)_i$ with

$$H = (I + m M^{-1} M^{-1\dagger} m^\dagger)^{-\frac{1}{2}}. \tag{2.15}$$

Substituting this form of 10_i in Eq. (2.13), one can write down the light quark and light lepton mass matrices as [19]

$$M_U = H^T M_U^0 H, \tag{2.16}$$

$$M_D = M_D^0 H, \tag{2.17}$$

$$M_L = H^T M_L^0, \tag{2.18}$$

$$M_N = M_N^0, \tag{2.19}$$

$$M_R = M_R^0, \tag{2.20}$$

where $M_{U,D}$ are the up-type and down-type quark mass matrices, M_L is the charged lepton mass matrix, M_N is the Dirac-type neutrino mass matrix, and M_R is the right-handed neutrino Majorana mass matrix. In writing these mass matrices we have defined [35]

$$M_U^0 = \langle 5_H \rangle Y^5 + \langle 45_H \rangle Y^{45}, \tag{2.21}$$

$$M_D^0 = \langle \bar{5}_H \rangle Y^{\bar{5}} + \langle \overline{45}_H \rangle Y^{\overline{45}}, \tag{2.22}$$

$$M_L^0 = \langle \bar{5}_H \rangle Y^{\bar{5}T} - 3 \langle \overline{45}_H \rangle Y^{\overline{45}T}, \tag{2.23}$$

$$M_N^0 = \langle 5_H \rangle Y^1, \tag{2.24}$$

$$M_R^0 = v_R Y_R^0. \tag{2.25}$$

Note that all matrices in Eqs. (2.21)–(2.24) are general complex, while M_R^0 in Eq. (2.25) is complex symmetric. (M_U^0 has symmetric contributions from $\langle 5_H \rangle$ as well as antisymmetric contributions from $\langle 45_H \rangle$, with the sum being neither symmetric nor antisymmetric).

The Hermitian matrix H in Eq. (2.15) can be written as $H = U^\dagger \mathrm{diag}\{\epsilon_1, \epsilon_2, \epsilon_3\} U$, with U being a unitary matrix and ϵ_i's being real and positive ($i = 1, 2, 3$). Substituting this form of H in Eqs. (2.16)–(2.18) and redefining the quark and lepton fields, one can absorb the unitary matrix U into the nonhierarchical matrices $M_{U,D,L}^0$ without affecting the numerical results. Thus, we choose $H = \mathrm{diag}\{\epsilon_1, \epsilon_2, \epsilon_3\}$. A hierarchy $\epsilon_1 \ll \epsilon_2 \ll \epsilon_3 \sim 1$ can be generated within the model by arranging for unequal mixings between the 10_i and 10_α for different families. For example, for the third family, we may take $M_3 \gg m_3$ (ignoring generation mixing for simplicity of explaining) while for the second and first families we may take $M_2 \ll m_2$ and $M_1 \lll m_1$; see Eq. (2.15) [19]. We shall set $\epsilon_3 = 1$, since this parameter is of order one, and redefining other parameters of the theory enables this choice. Consequently, we will choose

$$H = \mathrm{diag}\{\epsilon_1, \epsilon_2, 1\} \tag{2.26}$$

for our analysis.

The MSSM up-type Higgs doublet H_u that remains light to low energies is a linear combination of up-type doublets from the 5_H, 45_H, and other possible up-type Higgs doublets present in the $SU(5)$ model. Similarly the light MSSM field H_d is a linear combination of down-type Higgs doublets from $\bar{5}_H$, $\overline{45}_H$, and other possible down-type Higgs doublets in the model. An example of such additional up-type and down-type Higgs doublets is a pair of $5'_H + \bar{5}'_H$ fields with no Yukawa couplings to the fermions. We then have

$$H_u = \alpha_u h_5^u + \beta_u h_{45}^u + \sum_i \gamma_i^u h_i'^u, \tag{2.27}$$

$$H_d = \alpha_d h_{\bar{5}}^d + \beta_d h_{\overline{45}}^d + \sum_i \gamma_i^d h_i'^d \tag{2.28}$$

with $|\alpha_u|^2 + |\beta_u|^2 + \sum_i |\gamma_i^u|^2 = 1 = |\alpha_d|^2 + |\beta_d|^2 + \sum_i |\gamma_i^d|^2$. Here $h_5^u = (1, 2, \frac{1}{2}) \subset 5_H$, $h_{45}^u = (1, 2, \frac{1}{2}) \subset 45_H$, $h_{\bar{5}}^d = (1, 2, -\frac{1}{2}) \subset \bar{5}_H$, and $h_{\overline{45}}^d = (1, 2, -\frac{1}{2}) \subset \overline{45}_H$, where the quantum numbers under the SM gauge symmetry are indicated. The fields $h_i'^u$ and $h_i'^d$ are $(1, 2, \frac{1}{2})$ and $(1, 2, -\frac{1}{2})$ fields from additional Higgs multiplets, such as $5'_H + \bar{5}'_H$ pairs. All fields orthogonal to H_u and H_d remain superheavy. The VEVs of the doublet components of the various fields are related to the VEVs v_u and v_d of the MSSM fields H_u and H_d as

$$v_5 = \alpha_u^* v_u, \qquad v_{45} = \beta_u^* v_u, \tag{2.29}$$

$$v_{\bar{5}} = \alpha_d^* v_d, \qquad v_{\overline{45}} = \beta_d^* v_u. \tag{2.30}$$

Substituting these relations, one can rewrite the effective mass matrices Eqs. (2.16)–(2.20) for the fermions as

$$M_U = v_u H^T Y_U^0 H \equiv v_u Y_U, \tag{2.31}$$

$$M_D = v_d \epsilon_4 Y_D^0 H \equiv v_d Y_D, \tag{2.32}$$

$$M_L = v_d \epsilon_4 H^T Y_L^0 \equiv v_d Y_L, \tag{2.33}$$

$$M_N = v_u Y_N^0 \equiv v_u Y_N, \tag{2.34}$$

$$M_R = v_R Y_R^0 \equiv v_R Y_R. \tag{2.35}$$

Here Y_U^0, Y_D^0, etc., are the bare Yukawa coupling matrices derived from Eqs. (2.21)–(2.24), using the definitions given in Eq. (2.30),

$$Y_U^0 = \alpha_u^* Y^5 + \beta_u^* Y^{45}, \tag{2.36}$$

$$Y_D^0 = \alpha_d^* Y^{\bar{5}} + \beta_d^* Y^{\overline{45}}, \tag{2.37}$$

$$Y_L^0 = \alpha_d^* Y^{\bar{5}T} - 3\beta_d^* Y^{\overline{45}T}, \tag{2.38}$$

$$Y_N^0 = \alpha_u^* Y^1. \tag{2.39}$$

Thus, we see that the effective Yukawa coupling matrices of the quarks and leptons with the MSSM Higgs fields as given in Eqs. (2.1)–(2.5) are generated. The bare Yukawa couplings $Y_{U,D,L,N,R}^0$ in these equations will be treated as random variables obeying Gaussian distributions in our numerical analysis. The parameter ϵ_4 appearing in Eqs. (2.32) and (2.33) arises from the Higgs doublet mixing expressed in terms of $(\alpha_{u,d}, \beta_{u,d})$. To realize values of ϵ_4 in the range $\epsilon_4 = (0.04 - 0.1)$ as our fits would prefer, it is sufficient to take α_d and β_d somewhat smaller than one. Unitarity of the Higgs mixing matrix is maintained due to the presence of additional Higgs doublets such as $5'_H + \bar{5}'_H$ in the model. The model also has $\tan\beta = v_u/v_d$ as an input parameter. A relation between the $\tan\beta = v_u/v_d$ and ϵ_4 can be obtained from Eqs. (2.31) and (2.32),

$$\epsilon_4 \simeq \frac{m_b}{m_t} \tan\beta \frac{(Y_U^0)_{33}}{|(\overrightarrow{d_0})_3|}, \tag{2.40}$$

where we have defined $(\overrightarrow{d_0})_3 = \{(Y_D^0)_{13}, (Y_D^0)_{23}, (Y_D^0)_{33}\}$. Note that to set $\epsilon_3 = 1$ which we have adopted, we redefine

ϵ_4 in Eqs. (2.32) and (2.33), and also redefine v_u in Eq. (2.31).

Since the masses of the vectorlike fermions are of the order of GUT scale, any effect of these particles at low energies will be suppressed by a factor of $1/M_{\rm GUT}$, except for the dimension four fermion mass operators as discussed in the text. Hence their presence does not change the phenomenology of the MSSM or the Higgs boson mass. Even though the superheavy vectorlike fermions decouple, they may leave imprints on the SUSY flavor structure at low energies. However, SUSY models with large superpartner masses or gauge-mediated SUSY breaking models can potentially suppress any such flavor violating effects.

As noted previously, there are other ways of generating the Yukawa structure shown in Eqs. (2.1)–(2.5) by assuming $U(1)$ flavor symmetry that distinguishes the three families of 10_i [8], and/or the first family of $\bar{5}_1$ from $\bar{5}_{2,3}$ [23,24], by hypothesizing that the 10_i-plets are composite [20,36], or by postulating extra dimensions [25,26,28]. Another interesting class of models proposed recently in Refs. [37,38] has a very similar structure for the mass matrices, which we shall not investigate here. We do analyze the flavor $U(1)$ models as special cases of the general class of models described here, which are described next.

B. $SU(5)$-inspired models with $U(1)$ flavor symmetry

In this subsection we briefly describe a class of $SU(5)$-inspired models with $U(1)$ flavor symmetry. Models of this type can explain the hierarchical structure in the fermion masses and mixings by using the Fraggatt-Nielsen mechanism [22]. Smaller entries in the mass matrices are induced as higher dimensional operators suppressed by differing inverse powers of a fundamental mass scale. Assigning different charges to different families will lead to a hierarchy in masses and mixings.

The models we study here are inspired by SUSY $SU(5)$ unification—in the sense that the flavor $U(1)$ charge assignment will be compatible with $SU(5)$—but we can work just within the framework of MSSM. We shall use the language of $SU(5)$, however, for simplicity. The three fermion families are assigned to $10_i + \bar{5}_i$, and we include three families of SM singlet 1_i (ν_i^c) fields for the seesaw mechanism. In order to reproduce the observed hierarchical structure in fermion masses, we make specific $U(1)$ charge assignment to the fermion fields as shown in Table I. The integer charges q_1, q_2, and p are left unspecified in the table, and two different choices will be presented below.

In these models, the $U(1)$ flavor symmetry is broken by a single parameter $\epsilon = \langle S\rangle/M_*$, where $\langle S\rangle$ is the VEV of an $SU(5)$ singlet flavon field S with $U(1)$ charge -1 and $M_* > M_{\rm GUT}$ is a fundamental scale such as the string scale. The Yukawa superpotential contains higher dimensional terms suppressed by inverse powers of M_*, with coefficients which are all of order one. These couplings have the form

TABLE I. The flavor $U(1)$ charge assignment of the fermion fields in $SU(5)$ notation. The Yukawa matrices of Eqs. (2.1)–(2.5) will be induced with the choice $q_1 = 1$, $q_2 = p = 0$. Yukawa couplings given in Eqs. (2.43)–(2.45) will result with the choice $q_1 = 2$, $q_2 = 1$, $p = 0$, 1, or 2, corresponding to large, medium, and small $\tan\beta$. These models also contain a flavon field S with $U(1)$ charge of -1 that acquires a VEV. The Higgs doublets H_u and H_d of MSSM are neutral under this $U(1)$.

Field	$U_A(A)$ charge
10_1, 10_2, 10_3	$2q_1$, q_1, 0
$\bar{5}_1$, $\bar{5}_2$, $\bar{5}_3$	q_2+p, p, p
1_1, 1_2, 1_3	q_2, 0, 0

$$\mathcal{W}_Y \supset Y^u_{ij} Q_i u^c_j H_u \left(\frac{S}{M_*}\right)^{n^u_{ij}} + Y^d_{ij} Q_i d^c_j H_d \left(\frac{S}{M_*}\right)^{n^d_{ij}} + Y^\ell_{ij} L_i e^c_j H_d \left(\frac{S}{M_*}\right)^{n^\ell_{ij}} + Y^\nu_{ij} L_i \nu^c_j H_u \left(\frac{S}{M_*}\right)^{n^\nu_{ij}} + v_R Y^R_{ij} \nu^c_i \nu^c_j \left(\frac{S}{M_*}\right)^{n^{\nu^c}_{ij}}. \tag{2.41}$$

Here the integers n^u_{ij} etc are chosen such that the corresponding Yukawa coupling Y^u_{ij} is charge neutral. The couplings Y^u_{ij}, etc., are all taken to be of order unity. Still hierarchical masses and mixings are induced since the (ij) entry in the mass matrix has a suppression factor $\epsilon^{n_{ij}}$.

In our first flavor $U(1)$ model we choose the $U(1)$ charges of Table I to be $\{q_1 = 1, q_2 = 0, p = 0\}$ [8]. In this case the Yukawa coupling matrices will have the same form as in Eqs. (2.1)–(2.5). Note that in this model the three families of $\bar{5}_i$ are neutral under $U(1)$, while the 10_i carry differing charges given as (2,1,0). Since the $U(1)$ symmetry is broken by a single parameter, the Hermitian matrix H appearing in Eqs. (2.1)–(2.5) is now given by

$$H = \begin{pmatrix} \epsilon^2 & 0 & 0 \\ 0 & \epsilon & 0 \\ 0 & 0 & 1 \end{pmatrix}. \tag{2.42}$$

The only difference from the general model of the previous subsection is that here $\epsilon_2 \equiv \epsilon$ and $\epsilon_1 = \epsilon^2$.[1] This model will be analyzed separately, with the assumption that the Yukawa couplings entering Eq. (2.41) are random variables taking Gaussian distributions. The light neutrino mass matrix retains exactly the same structureless pattern as before, since the ν^c fields as well as the L_i fields are all neutral under the $U(1)$. If the model is embedded in $SU(5)$ minimally, the wrong relation

[1]Strictly, $\epsilon_1 = O(1)\epsilon^2$, but this $O(1)$ coefficient may be absorbed into other $O(1)$ Yukawa couplings, which is what we shall do.

$Y_L = Y_D^T$ would result. This would require the extension of the scalar sector by a $45_H + \overline{45}_H$ pair. As before, the parameter ϵ_4 has the same definition as in Eqs. (2.1)–(2.5), and such models have two hierarchical parameters $\{\epsilon, \epsilon_4\}$.

A second flavor $U(1)$ model is obtained by the choice of $U(1)$ charges in Table I as $\{q_1 = 2, q_2 = 1, p = 0, 1, \text{or } 2\}$ along with the charges of the scalar fields given by $\{H_u, H_d, S\} = \{0, 0, -1\}$. Here the first family $\bar{5}_1$ has a shifted charge compared to $\bar{5}_{2,3}$. This is the only difference of this model compared to the first flavor $U(1)$ model just discussed. Such a model has been studied in Refs. [23,24], where the Yukawa coupling matrices written in the basis $f_i^c (Y_f)_{ij} f_j$ are shown to take the form

$$Y_U \sim \begin{pmatrix} \epsilon^8 & \epsilon^6 & \epsilon^4 \\ \epsilon^6 & \epsilon^4 & \epsilon^2 \\ \epsilon^4 & \epsilon^2 & 1 \end{pmatrix}, \qquad Y_D \sim \epsilon^p \begin{pmatrix} \epsilon^5 & \epsilon^3 & \epsilon \\ \epsilon^4 & \epsilon^2 & 1 \\ \epsilon^4 & \epsilon^2 & 1 \end{pmatrix}, \tag{2.43}$$

$$Y_L \sim \epsilon^p \begin{pmatrix} \epsilon^5 & \epsilon^4 & \epsilon^4 \\ \epsilon^3 & \epsilon^2 & \epsilon^2 \\ \epsilon & 1 & 1 \end{pmatrix}, \qquad Y_N \sim \epsilon^p \begin{pmatrix} \epsilon^2 & \epsilon & \epsilon \\ \epsilon & 1 & 1 \\ \epsilon & 1 & 1 \end{pmatrix}, \tag{2.44}$$

$$Y_R \sim \begin{pmatrix} \epsilon^2 & \epsilon & \epsilon \\ \epsilon & 1 & 1 \\ \epsilon & 1 & 1 \end{pmatrix}, \quad \mathcal{Y}_\nu \sim \epsilon^{2p} \begin{pmatrix} \epsilon^2 & \epsilon & \epsilon \\ \epsilon & 1 & 1 \\ \epsilon & 1 & 1 \end{pmatrix}. \tag{2.45}$$

Here $\mathcal{Y}_\nu$ determines the light neutrino mass matrix via the seesaw relation $M_\nu = \mathcal{Y}_\nu v_u^2 / v_R$. The integer p is allowed to take three different values, $p = 0$, 1, or 2, corresponding to large, medium, and small values of $\tan\beta$. In Eqs. (2.43)–(2.45), each matrix element has an $O(1)$ coefficient c_{ij}^f that is not explicitly shown. These entries are taken to be of order unity. For our statistical analysis of the model, we shall take these c_{ij}^f to be random variables obeying uncorrelated Gaussian distributions. One clearly sees that although the charged fermion mass matrices here are quite similar to the previously discussed models, the light neutrino mass matrix is significantly different. Unlike the previous cases, it is no longer given by a matrix with order unity entries everywhere; rather it has somewhat of a hierarchical structure. In this model, it is possible to correct the $SU(5)$ relation $M_L = M_D^T$ via higher dimensional operators involving the 24_H field, and therefore, a parameter analogous to ϵ_4 is not required. As we shall see, a good fit to all data is obtained in this model with a single hierarchy parameter ϵ.

III. STATISTICAL ANALYSIS OF FLAVOR PARAMETERS IN $SU(5)$-BASED MODELS

In this section we perform a statistical analysis of the general class of unified theories based on $SU(5)$. The general model described in Sec. II A contains three hierarchical input parameters $\{\epsilon_1, \epsilon_2, \epsilon_4\}$ as well as $\tan\beta$ in the flavor sector. In addition, these models have five complex Yukawa coupling matrices [see Eqs. (2.1)–(2.5)], the elements of which are treated as uncorrelated random variables with Gaussian distributions. After a detailed analysis of this general setup, we repeat the analysis for the two $SU(5)$-inspired flavor $U(1)$ variants. These variants have either two sets of hierarchical parameters $\{\epsilon, \epsilon_4\}$ or a single parameter ϵ.

The primary goal of this section is to investigate how well the theoretical predictions of this class of models agree with the experimentally observed quantities on average. We perform a Monte Carlo simulation and derive the theoretical expectations for these models. We start with the MSSM Yukawa coupling matrices given in Eqs. (2.1)–(2.5). As noted before, the matrices Y_F^0 in Eqs. (2.1)–(2.5) are random matrices with all elements of order $O(1)$. The matrices Y_F^0 for $F = U, D, L, N$ are of the Dirac-type and in general complex matrices. The right-handed neutrino Yukawa coupling matrix Y_R^0 in Eq. (2.5) is of the Majorana-type which is complex symmetric. We assume that each of these matrix elements is a random variable independent of other elements. The probability distributions of the matrix elements are assumed to be completely independent of the hierarchical model parameters $\{\epsilon_1, \epsilon_2, \epsilon_4\}$. Basis independence as well as the absence of correlation between various matrix elements determines uniquely the probability measures for these random variables to be Gaussian [16,18],

$$dY_{\rm D}^0 = \prod_{ij} dY_{ij}^0 e^{-|Y_{ij}^0|^2},$$
$$dY_{\rm M}^0 = \prod_i dY_{ii}^0 e^{-|Y_{ii}^0|^2} \prod_{i<j} dY_{ij}^0 e^{-2|Y_{ij}^0|^2}. \tag{3.1}$$

Here the subscripts D and M represent Dirac-type and Majorana-type, respectively. These measures are defined up to a scale factor e^{-c}, which has been set equal to 1. (When Gaussian distributions are applied to mass matrices, this scale factor can be used to fix the overall scale of the VEV; see Ref. [18] for details.) From Eq. (3.1), all the elements of a general complex random matrix are independently generated with a Gaussian distribution of variance 0.5 for both the real and the imaginary parts separately. Similarly, for the complex symmetric random matrix, the real and imaginary parts are generated independently with a Gaussian distribution of variance 0.5 and 0.25 for diagonal and off-diagonal entries, respectively.

TABLE II. Observables in the charged fermion sector at the M_Z scale taken from Ref. [39]. For quantities with asymmetrical error bars, we have symmetrized and presented the experimental central values with associated 1σ uncertainties. The fermion masses are given by the relations $m_i(M_Z) = v y_i^{SM}(M_Z)$, with $v = 174$ GeV.

Yukawa couplings and CKM parameters	$\mu = M_Z$
$y_u/10^{-6}$	6.65 ± 2.25
$y_c/10^{-3}$	3.60 ± 0.11
y_t	0.9860 ± 0.00865
$y_d/10^{-5}$	1.645 ± 0.165
$y_s/10^{-4}$	3.125 ± 0.165
$y_b/10^{-2}$	1.639 ± 0.015
$y_e/10^{-6}$	2.79475 ± 0.0000155
$y_\mu/10^{-4}$	5.89986 ± 0.0000185
$y_\tau/10^{-2}$	1.00295 ± 0.0000905
θ_{12}^{CKM}	0.22735 ± 0.000072
$\theta_{23}^{CKM}/10^{-2}$	4.208 ± 0.064
$\theta_{13}^{CKM}/10^{-3}$	3.64 ± 0.13
δ^{CKM}	1.208 ± 0.054

The class of models with Yukawa matrices given in Eqs. (2.1)–(2.5) has three input parameters, ϵ_i ($i = 1, 2, 4$) and 84 random variables (72 in four general complex random matrices and 12 in one random complex symmetric matrix). In this section we present a Monte Carlo analysis of these models adopting the Gaussian measure for the random matrix elements. The parameters ϵ_i are, however, not random; instead they are fixed by χ^2-function minimization. We have seen previously that these parameters do not enter in the neutrino sector. Thus, in order to fix the numerical values of these parameters we only include in the χ^2 minimization the observables in the charged fermion sector. The minimization is carried out at the GUT scale with three input parameters to fit 13 observables.

To perform the χ^2 minimization at the GUT scale we take the experimentally observed values of the charged fermion observables at the M_Z scale from Ref. [39]. These values are quoted in Table II. We use the renormalization group running factors corresponding to MSSM, $\eta_i = m_i(M_{GUT})/m_i(M_Z)$, taken from Ref. [40] for the evolution of the Yukawa couplings from the M_Z scale to the GUT scale. These running factors are listed in Table III. We perform the Monte Carlo analysis for two values of the parameter $\tan\beta$, 10 and 50. The Yukawa couplings at the GUT scale are obtained from the couplings determined at $\mu = M_Z$ with the help of these renormalization running factors by using the relations $y_{u_i}^{MSSM}(M_{GUT}) = y_{u_i}^{SM}(M_Z)\eta_{u_i}/\sin\beta$ for up-type quarks and $y_{d_i,e_i}^{MSSM}(M_{GUT}) = y_{d_i,e_i}^{SM}(M_Z)\eta_{d_i,e_i}/\cos\beta$ for down-type quarks and charged leptons. We also run the Cabibbo-Kobayashi-Maskawa (CKM) mixing parameters from M_Z to the GUT scale using the MSSM renormalization group equations [41,42]. The renormalization running factors of the CKM matrix elements are presented in Table III. The Yukawa couplings and the CKM mixing parameters at the GUT scale are presented in Table IV. For the associated 1σ uncertainties of these observables at the GUT scale, we take the same percentage uncertainty with respect to the central value of each quantity as that at the M_Z scale. For the charged lepton Yukawa couplings, a relative uncertainty of 1% is assumed, instead of smaller experimental statistical errors, in order to take into account the theoretical uncertainties such as SUSY and GUT scale threshold effects.

TABLE III. Renormalization group running factors for the masses, $\eta_i = m_i(M_{GUT})/m_i(M_Z)$ (taken from Ref. [40]). These values are obtained with two-loop MSSM renormalization group evolution with appropriate one-loop matching conditions. In the last row the renormalization group running factors $\eta_{ij}^{CKM} = V_{ij}(M_{GUT})/V_{ij}(M_Z)$ of the CKM matrix elements are listed, which are obtained by evolving the RGEs for these parameters [41,42] from low energy to M_{GUT}.

$\tan\beta$	10	50
(η_u, η_c, η_t)	(0.385, 0.381, 0.536)	(0.377, 0.382, 0.551)
(η_d, η_s, η_b)	(0.241, 0.236, 0.273)	(0.175, 0.181, 0.211)
$(\eta_e, \eta_\mu, \eta_\tau)$	(0.583, 0.583, 0.585)	(0.423, 0.423, 0.442)
$(\eta_{us}^{CKM}, \eta_{cb}^{CKM}, \eta_{ub}^{CKM})$	(0.999, 0.890, 0.890)	(0.999, 0.826, 0.826)

TABLE IV. Input values at M_{GUT} used in our fits. Central values and 1σ errors are quoted. For Yukawa couplings, these numbers are found with the help of Tables II and III and by using the equations $y_{u_i}^{MSSM}(M_{GUT}) = y_{u_i}^{SM}(M_Z)\eta_{u_i}/\sin\beta$ for up-type quarks and $y_{d_i,e_i}^{MSSM}(M_{GUT}) = y_{d_i,e_i}^{SM}(M_Z)\eta_{d_i,e_i}/\cos\beta$ for down-type quarks and charged leptons. For the charged lepton Yukawa couplings, a relative uncertainty of 1% is assumed, instead of smaller experimental statistical errors, in order to take into account the theoretical uncertainties from threshold effects. For the CKM mixing parameters, we evolve the quantities from low scale to M_{GUT} by using the RGEs provided in Refs. [41,42].

Yukawa couplings and CKM mixing parameters	$\tan\beta = 10$ (at $\mu = M_{GUT}$)	$\tan\beta = 50$ (at $\mu = M_{GUT}$)
$y_u/10^{-6}$	2.57 ± 0.86	2.51 ± 0.84
$y_c/10^{-3}$	1.37 ± 0.04	1.37 ± 0.04
$y_t/10^{-1}$	5.31 ± 0.04	5.43 ± 0.04
$y_d/10^{-4}$	0.39 ± 0.04	1.44 ± 0.14
$y_s/10^{-3}$	0.74 ± 0.03	2.84 ± 0.14
$y_b/10^{-2}$	4.49 ± 0.04	17.29 ± 0.15
$y_e/10^{-5}$	1.63 ± 0.01	5.91 ± 0.05
$y_\mu/10^{-3}$	3.45 ± 0.03	12.49 ± 0.12
$y_\tau/10^{-2}$	5.89 ± 0.05	22.21 ± 0.22
$\lvert V_{us}\rvert/10^{-2}$	22.53 ± 0.07	22.53 ± 0.07
$\lvert V_{cb}\rvert/10^{-2}$	3.74 ± 0.05	3.47 ± 0.05
$\lvert V_{ub}\rvert/10^{-3}$	3.24 ± 0.11	3.00 ± 0.10
η_W	0.35 ± 0.01	0.35 ± 0.01

TABLE V. Model parameters determined by χ^2 minimization for the $SU(5)$-based GUTs defined in Eqs. (2.1)–(2.5).

$\tan\beta$	10	50
ϵ_1	0.00181 ± 0.00010	0.00169 ± 0.00009
ϵ_2	0.0388 ± 0.00222	0.03659 ± 0.00215
ϵ_4	0.04055 ± 0.00229	0.15716 ± 0.00894

With these GUT scale inputs, using Eqs. (2.1)–(2.5), we perform χ^2 minimization by treating ϵ_1, ϵ_2, and ϵ_4 as parameters and fit the data in the charged fermion sector. Here $n_{\rm obs} = 13$ is the number of observables, with three parameters to fit them. The elements of the random matrices pick up random values independently according to Gaussian distribution. For our analysis the error, pull, and χ^2 function are defined as follows:

$$\sigma_i = \sqrt{\sigma_{i\rm th}^2 + \sigma_{i\,\rm exp}^2},$$
$$P_i = \frac{O_{i\rm th} - E_{i\,\rm exp}}{\sigma_i},$$
$$\chi^2 = \sum_i P_i^2, \tag{3.2}$$

where $\sigma_{i\rm th}$ and $\sigma_{i\,\rm exp}$ represent the theoretical standard deviation (TSD) and experimental 1σ uncertainty, respectively, and $O_{i\rm th}$, $E_{i\,\rm exp}$, and P_i represent the theoretical mean value (TMV), experimental central value (ECV), and pull of an observable i.

We find the minimum with $\chi^2/n_{\rm obs} \sim 1$ along with the model parameters shown in Table V. The best fit values of the observables obtained with these fixed model parameters resulting from our Monte Carlo optimization are shown in Table VI. In Fig. 1 we plot the histogram distributions of the observables in the quark and the charged lepton sectors corresponding to the fixed model parameters given in Table V for the case where $\tan\beta = 10$ (plots for the case $\tan\beta = 50$ are similar). In producing these distributions we have taken the sample size to be 10^4 and chose the bin size (N bins) to be 50.

The blue plots in Fig. 1 show histograms of the theoretical distributions of the up-type quark Yukawa couplings. Overlaid on these distributions are the experimental values of these couplings. We find very good agreement between theoretical expectations and observations. Among all the charged fermions, the eigenvalue spectrum of the up-type quarks shows the most hierarchical structure which is nicely reproduced. This is not surprising, as the stronger hierarchy is built into the model; see Eqs. (2.1)–(2.5).

For the down-type quark Yukawa couplings, theoretical distributions are shown in green in Fig. 1. Overlaid on these distributions are the experimental values of these parameters. These are in good agreement with observations for down quark and bottom quark, whereas for the strange quark, the theoretical mean value tends to be a little higher than the experimentally measured value, but it is still within the acceptable range. In the eigenvalue spectrum of charged leptons, which is shown in pink in Fig. 1, the theoretical mean value for the muon Yukawa coupling tends to be a little lower than the experimental central value. The reason for these small discrepancies can be understood from the approximate relations $\frac{y_s}{y_b} \sim \epsilon_2$ and $\frac{y_\mu}{y_\tau} \sim \epsilon_2$ present in the model. At the GUT scale one has roughly $y_b \sim y_\tau$, which implies within the model $y_s \sim y_\mu$. This is why the histograms of Yukawa couplings for both strange-quark and muon Yukawa couplings are almost identical with

TABLE VI. χ^2 best fit values of the observables for the $SU(5)$-based GUTs defined in Eqs. (2.1)–(2.5) with the fixed model parameters given in Table V. The best fit values shown in this table correspond to $\chi^2/n_{\rm obs} = 1.13$ and 1.12 for $\tan\beta = 10$ and 50, respectively. Here TMV = theoretical mean value, TSD = theoretical standard deviation, ECV = experimental central value, and pull is defined in Eq. (3.2).

	TMV $\pm$ TSD		$\frac{\rm TMV}{\rm ECV}$		Pull	
Observables	$\tan\beta = 10$	$\tan\beta = 50$	$\tan\beta = 10$	$\tan\beta = 50$	$\tan\beta = 10$	$\tan\beta = 50$
$y_u/10^{-6}$	7.23 ± 7.76	6.39 ± 6.93	2.81	2.54	0.59	0.55
$y_c/10^{-3}$	2.55 ± 2.53	2.26 ± 2.37	1.85	1.64	0.46	0.37
y_t	0.88 ± 0.46	0.89 ± 0.46	1.67	1.63	0.77	0.74
$y_d/10^{-4}$	0.64 ± 0.33	2.3 ± 1.23	1.61	1.62	0.73	0.73
$y_s/10^{-3}$	2.10 ± 0.77	7.59 ± 2.79	2.83	2.67	1.75	1.69
$y_b/10^{-1}$	0.67 ± 0.19	2.61 ± 0.76	1.50	1.51	1.13	1.15
$y_e/10^{-4}$	0.64 ± 0.34	2.34 ± 1.22	3.96	3.96	1.42	1.42
$y_\mu/10^{-3}$	2.10 ± 0.75	7.63 ± 2.74	0.60	0.61	−1.79	−1.76
$y_\tau/10^{-1}$	0.67 ± 0.19	2.59 ± 0.76	1.14	1.16	0.42	0.48
$\lvert V_{us}\rvert/10^{-2}$	8.17 ± 7.80	8.07 ± 7.87	0.36	0.35	−1.83	−1.83
$\lvert V_{cb}\rvert/10^{-2}$	6.15 ± 6.37	5.99 ± 6.34	1.64	1.72	0.37	0.39
$\lvert V_{ub}\rvert/10^{-3}$	3.42 ± 3.67	3.23 ± 3.75	1.05	1.07	0.04	0.06
η_W	0.05 ± 3.13	0.05 ± 2.59	0.14	0.14	−0.09	−0.11

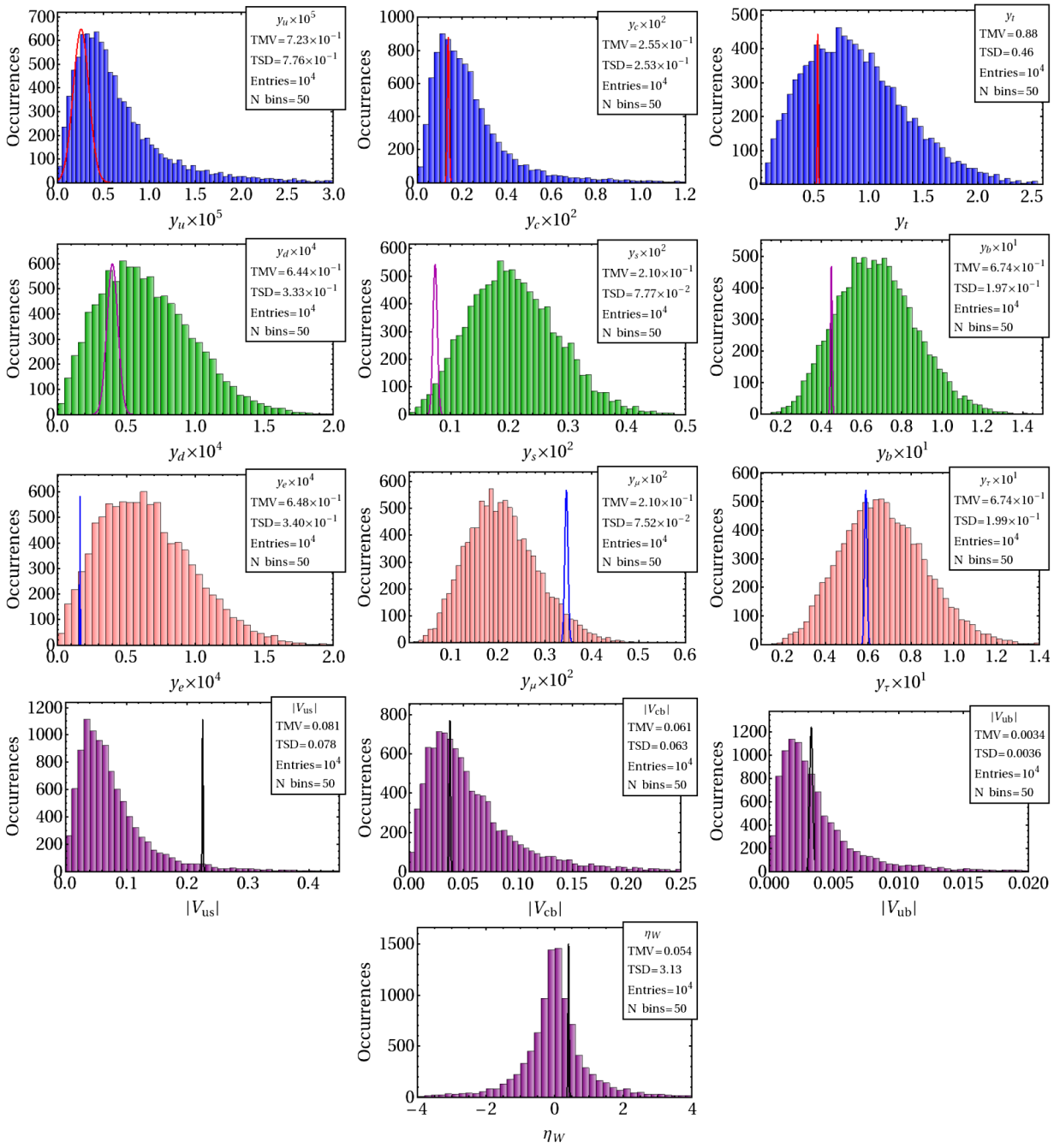

FIG. 1. Histogram plots showing the distributions of the observables in the charged fermion sector. Blue (green, pink, and purple) plots are the theoretical distributions of the up-type quarks (down-type quarks, charged leptons, and CKM mixing parameters) according to the $SU(5)$-based GUTs with 10^4 occurrences for the case of $\tan\beta = 10$ corresponding to the model parameters given in Table V. Red (magenta, blue, and black) curves represent the corresponding experimental 1σ uncertainty range. For the charged leptons, a relative uncertainty of 1% is assumed in order to take into account theoretical uncertainties arising from SUSY and GUT scale threshold effects. The number of bins (N bins) is chosen to be 50.

approximately the same theoretical mean values, but observation dictates $y_s \sim 4y_\mu$ at the GUT scale. This small discrepancy, inherent to these models, is still not major and is within the acceptable range.

The probability distributions of the CKM parameters are shown in purple in Fig. 1. Overlaid on these distributions are the experimental values of these observables. These distributions[2] are also in very good agreement with data. The theoretical distribution for V_{us} has a mean value that

[2]Similar distributions for the CKM parameters are obtained in Ref. [43] from a completely different statistical approach.

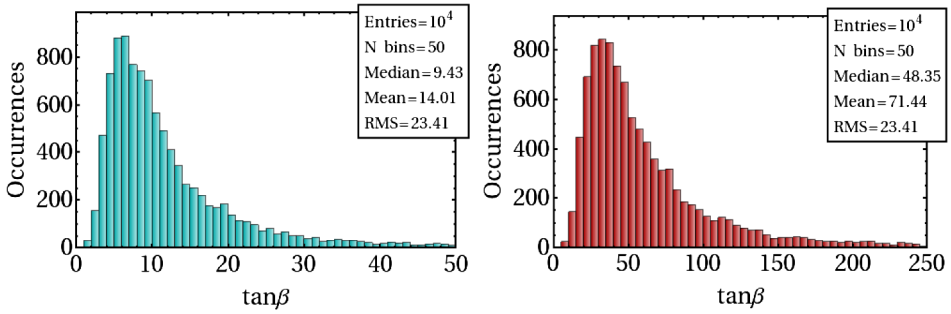

FIG. 2. Histograms showing theoretical distributions of $\tan\beta$ given by Eq. (2.40) for the $SU(5)$-based GUTs with a sample size of 10^4. The left plot corresponds to the case where $\tan\beta = 10$ and the right plot for $\tan\beta = 50$. The number of bins (N bins) is chosen to be 50.

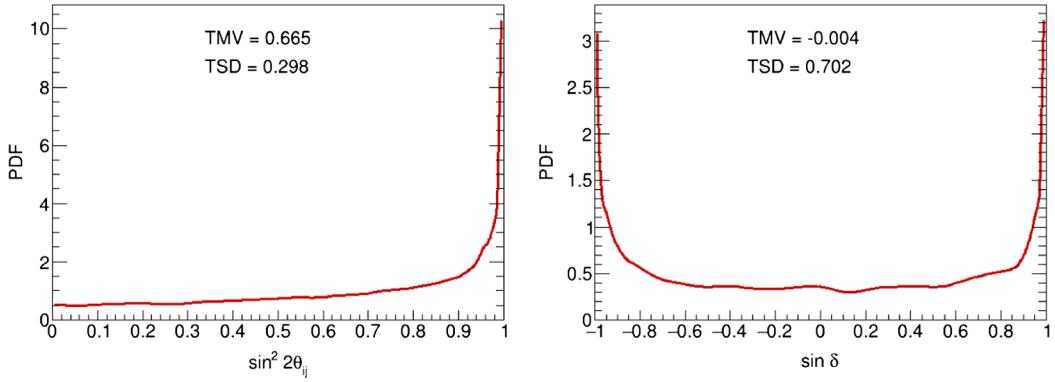

FIG. 3. Probability density plots for the neutrino mixing parameters for $SU(5)$-based GUTs. The left plot is for the mixing angles, $\sin^2 2\theta_{ij}$ for $(ij) = (12)$, (23), and (13), and the right plot is for the CP-violating parameter $\sin\delta$. In these probability density plots, the area under the curve within a certain range represents the probability of finding the quantity within that particular range. Here TMV = theoretical mean value, and TSD = theoretical standard deviation.

tends to be somewhat smaller than the experimental value. This feature may be understood since the model has $V_{us} \sim \epsilon_1/\epsilon_2$. It also predicts $y_d/y_s \sim 0.05 \sim \epsilon_1/\epsilon_2$, which makes V_{us} to peak around 0.05, rather than the observed value of ∼0.2. But there is still acceptable agreement.

We can do a consistency check for the value of $\tan\beta$ used. From Eq. (2.40) we have $\tan\beta \simeq \epsilon_4 m_t/m_b \frac{|(\vec{d}_0)_3|}{(Y^0_U)_{33}}$. Since $O(1)$ random variables are present in this equation, $\tan\beta$ in these models follows a distribution shown in Fig. 2. Both histograms have a long tail behavior with the mean values of the distributions being $\tan\beta = 14$ and 71.4, respectively. For histograms with such behavior, the median may be a better measure, which are $\tan\beta = 9.4$ and 48.3, respectively. We see broad consistency with the input values of $\tan\beta$ used in each case.

Since the small parameters ϵ_i do not enter into the neutrino sector, in the optimization process we did not include the neutrino observables. Once the model parameters are fixed as in Table V, one can include the neutrino sector in the sampling process and investigate how well the observed quantities in this sector are reproduced by these models. Since the matrix structure is the same as the ones considered in earlier works assuming anarchical hypothesis only in the neutrino sector [7,8], the histogram distributions of the neutrino observables should be similar, which is what we find. In Figs. 3 and 4 we present plots for the theoretical predictions of the neutrino observables. The theoretical average values of these observables resulting from the Monte Carlo analysis are shown in Table VII. The input values for neutrino observables are taken from Ref. [44] corresponding to the case of normal ordering of the neutrino mass spectrum. We restrict our analysis to normal ordering, since the random matrix structure for the neutrinos strongly prefers this over inverted ordering. In our Monte Carlo simulations we found a 95.6% probability for normal ordering and a 4.4% probability for inverted ordering, which is similar to the results of Ref. [18]. To ensure normal ordering, we assume $m_1 \leq m_2 < m_3$ and we put the constraint $r < 1$ ($r \equiv \Delta m^2_{\rm sol}/\Delta m^2_{\rm atm}$ with $\Delta m^2_{\rm sol} = m_2^2 - m_1^2$ and $\Delta m^2_{\rm atm} = m_3^2 - m_2^2$) in the sampling procedure.

In Fig. 3 we plot the probability density for the neutrino mixing parameters. The area under the curve in a probability density plot between any two values of the observable represents the probability of finding the observable within

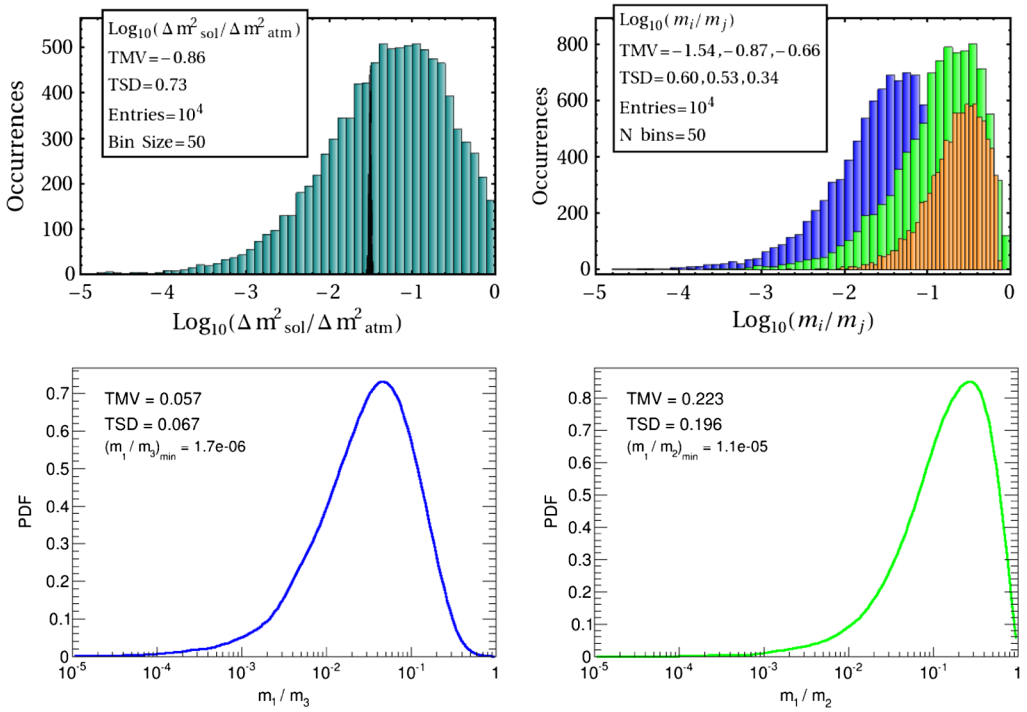

FIG. 4. Two histogram plots showing the theoretical distributions of $\log_{10}(\Delta m^2_{\rm sol}/\Delta m^2_{\rm atm})$ (upper left) and $\log_{10}(m_{ij}) = \log_{10}(m_i/m_j)$ [upper right; blue, green, and orange histograms are for $\log_{10}(m_1/m_3)$, $\log_{10}(m_1/m_2)$, and $\log_{10}(m_2/m_3)$, respectively]. The black curve in the upper left plot represents the experimental 1σ uncertainty range. The two bottom plots are the probability density functions for the neutrino mass ratios m_i/m_j (blue and green plots are for m_1/m_3 and m_1/m_2). In these probability density plots, the area under the curve within a certain range represents the probability of finding the quantity within that particular range. These plots are the results from our Monte Carlo analysis for the anarchical neutrino mass models with normal mass ordering. Here TMV = theoretical mean value, and TSD = theoretical standard deviation. For the two histogram distributions the number of bins is chosen to be 50 and for all the plots the sample size is taken to be 10^4.

that particular range, and the total area is normalized to unity. From these plots it is clear that for this class of models all the mixing parameters $\sin^2 2\theta_{ij}$ in the neutrino sector take preferentially large values. The CP-violating parameter $\sin\delta$ is peaked at its maximal values of ± 1. The preference of all the mixing parameters to be large is a consequence of the complete anarchical form of the neutrino mass matrix as their distributions are uniquely fixed by the invariant Haar measure.

In Fig. 4 we plot theoretical distributions of $\log_{10}(\Delta m^2_{\rm sol}/\Delta m^2_{\rm atm})$ and $\log_{10}(m_i/m_j)$. The upper left plot in Fig. 4 shows that the anarchic structure of the neutrino mass matrix prefers small values of the ratio of the two mass squared differences, r, and the theoretical mean value is quite close to the experimental central value. The upper right plot reveals that anarchy predicts mild hierarchy in the neutrino mass spectrum. The lower plots in Fig. 4 exhibit the probability densities for the two different neutrino mass ratios, m_1/m_3 and m_1/m_2. As can be seen, the ratio m_1/m_2 peaks around 0.3. Extreme small values of m_1 are strongly

TABLE VII. Theoretical sampling results of the $SU(5)$-based model obtained from Monte Carlo simulation in the neutrino sector. Experimental central values with associated 1σ uncertainties are also quoted taken from Ref. [44]. Here TMV = theoretical mean value, TSD = theoretical standard deviation, ECV = experimental central value, and pull is defined in Eq. (3.2). The theoretical results presented here are for a sample size of 10^4. The best fit values shown in this table correspond to $\chi^2/n_{\rm obs} = 0.66$.

Observables	ECV	1σ exp	TMV	TSD	$\frac{\rm TMV}{\rm EMV}$	Pull
$\frac{\Delta m^2_{\rm sol}}{\Delta m^2_{\rm atm}}$	0.031	0.001	0.135	0.186	4.37	0.56
$\sin^2\theta_{12}$	0.308	0.017	0.504	0.287	1.63	0.68
$\sin^2\theta_{23}$	0.3875	0.0225	0.501	0.290	1.29	0.39
$\sin^2\theta_{13}$	0.0241	0.0025	0.334	0.235	13.8	1.31

TABLE VIII. Model parameters determined by χ^2 minimization for the $SU(5)$-inspired $U(1)$ flavor symmetry models with two parameters.

$\tan\beta$	10	50
ϵ	0.02855 ± 0.00150	0.03847 ± 0.00215
ϵ_4	0.03909 ± 0.00220	0.14537 ± 0.00826

TABLE IX. χ^2 best fit values of the observables for the $SU(5)$-inspired $U(1)$ flavor symmetry models with two parameters. The fixed model parameters are given in Table VIII. The best fit values shown in this table correspond to $\chi^2/n_{\rm obs} = 1.44$ and 1.41 for $\tan\beta = 10$ and 50, respectively.

	TMV ± TSD		$\frac{\text{TMV}}{\text{ECV}}$		Pull	
Observables	$\tan\beta = 10$	$\tan\beta = 50$	$\tan\beta = 10$	$\tan\beta = 50$	$\tan\beta = 10$	$\tan\beta = 50$
$y_u/10^{-6}$	3.49 ± 3.89	4.96 ± 5.55	1.35	1.97	0.23	0.43
$y_c/10^{-3}$	2.08 ± 2.15	2.50 ± 2.57	1.51	1.82	0.32	0.43
y_t	0.88 ± 0.46	0.88 ± 0.46	1.65	1.63	0.76	0.74
$y_d/10^{-4}$	0.44 ± 0.23	1.92 ± 1.00	1.10	1.32	0.17	0.46
$y_s/10^{-3}$	1.90 ± 0.69	7.45 ± 2.71	2.56	2.62	1.67	1.69
$y_b/10^{-1}$	0.67 ± 0.19	2.42 ± 0.71	1.49	1.40	1.11	0.96
$y_e/10^{-4}$	0.44 ± 0.23	1.90 ± 1.00	2.69	3.21	1.41	1.31
$y_\mu/10^{-3}$	1.90 ± 0.75	7.38 ± 2.71	0.55	0.59	−2.24	−1.87
$y_\tau/10^{-1}$	0.68 ± 0.19	2.42 ± 0.70	1.15	1.09	0.42	0.28
$\lvert V_{us}\rvert/10^{-2}$	8.17 ± 7.80	6.81 ± 6.86	0.36	0.30	−2.68	−2.29
$\lvert V_{cb}\rvert/10^{-2}$	5.75 ± 5.93	6.19 ± 6.30	1.53	1.78	0.33	0.43
$\lvert V_{ub}\rvert/10^{-3}$	2.73 ± 3.03	2.81 ± 2.96	0.84	0.93	−0.16	−0.06
η_W	0.006 ± 2.509	0.003 ± 2.30	0.01	0.006	−0.15	−1.13

disfavored in this model. For example, $m_1/m_2 < 0.01$ will be favored only with a 4% probability.

A. Monte Carlo analysis of $SU(5)$-inspired $U(1)$ flavor models

1. Models with two parameters $\{\epsilon, \epsilon_4\}$

In this subsection, we present our Monte Carlo results for the $SU(5)$-inspired $U(1)$ flavor models with $U(1)$ charges chosen to be $\{q_1 = 1, q_2 = 0, p = 0\}$ as explained in Sec. II B. Models of this type have two parameters, $\{\epsilon, \epsilon_4\}$. The only modification needed compared to our general setup is in the charged fermions sector where the matrix H is given by Eq. (2.42). This set of models has one less parameter compared to the general model. We have performed a fit as before in this two parameter case, and the fitted model parameters are presented in Table VIII. From this table one finds $\epsilon \sim \lambda^2$, where $\lambda \sim 0.22$. With these fixed parameters, the corresponding best fit values of the observables are shown in Table IX, and the theoretical distributions of these quantities are presented in Fig. 8 in Appendix A 1. By comparing the fit results of Tables VI and IX one sees that a slightly better fit is obtained for the three parameter case compared to the analysis done here with one less parameter. In Table VI, all the observables are reproduced within 2σ error on average, whereas in Table IX, with one less parameter, two of the observables are in the $(2\text{–}3)\sigma$ range for the case of $\tan\beta = 10$ and for the case of $\tan\beta = 50$, and one of the observables is a little above the 2σ error on average. Since the neutrino sector is exactly the same for all these models belonging to $SU(5)$-based GUTs, the analysis in the previous subsection remains unchanged.

B. Monte Carlo analysis of $U(1)$ model with one parameter $\{\epsilon\}$

In this subsection we apply a Monte Carlo analysis to the $SU(5)$-inspired flavor symmetry model with the $U(1)$-flavor charge assignment of $\{q_1 = 2, q_2 = 1, p = 0, 1, 2\}$ as discussed in Sec. II B. As explained there, the matrix elements in Eqs. (2.43)–(2.45) have order one complex coefficients c_{ij}^f. We assume that the coefficients are random complex variables with a Gaussian distribution of variance 0.5 for both real and imaginary parts. For the off-diagonal terms of the complex symmetric matrix Y_R the coefficients have a variance of 0.25. We generate this unbiased set of random variables following Gaussian distribution in a manner similar to the one described earlier. By taking the sample size to be 10^4, we study the theoretical probability distributions of the observables in the fermion sector. We carry out the Monte Carlo analysis for three cases with $p = 0$, 1, 2 (corresponding to $\tan\beta = 55$, 25, 5, respectively) and present the values of the parameter ϵ that minimizes the χ^2 for each case. For these values of $\tan\beta$ the renormalization group equation (RGE) running factors are not given in Ref. [40], and hence we run the two loop MSSM RGEs [42,45] from low scale to the GUT scale.[3] We take the low scale central values of the observables from Table II of Ref. [39] at $\mu = 1$ TeV where the observables are converted to the $\overline{\rm DR}$ scheme, use the SUSY matching formula (without taking into account the threshold corrections) for the Yukawa couplings and evolve them up to the GUT scale, and use these values as inputs (shown in Table X)

[3]We also performed the running for the cases with $\tan\beta = 10$ and 50 and found consistency with Ref. [40] and hence the values presented in Table IV.

TABLE X. Experimental central values with associated 1σ uncertainties at the M_{GUT} scale used in our fits. The low scale central values of the observables are taken from Table II of Ref. [39] at $\mu = 1$ TeV. For the charged leptons, a relative uncertainty of 1% is assumed in order to take into account the theoretical uncertainties as for example SUSY threshold and GUT scale effects.

Yukawa couplings and CKM mixing parameters	$\tan\beta = 5$ (at $\mu = M_{GUT}$)	$\tan\beta = 25$ (at $\mu = M_{GUT}$)	$\tan\beta = 55$ (at $\mu = M_{GUT}$)
$y_u/10^{-6}$	2.98 ± 1.00	2.88 ± 0.96	2.96 ± 0.99
$y_c/10^{-3}$	1.45 ± 0.04	1.4 ± 0.04	1.44 ± 0.04
$y_t/10^{-1}$	5.43 ± 0.04	5.23 ± 0.04	5.85 ± 0.05
$y_d/10^{-4}$	0.24 ± 0.02	1.24 ± 0.12	3.55 ± 0.36
$y_s/10^{-3}$	0.48 ± 0.024	2.47 ± 0.12	7.04 ± 0.35
$y_b/10^{-2}$	2.73 ± 0.02	14.33 ± 0.12	49.61 ± 0.44
$y_e/10^{-4}$	0.10 ± 0.001	0.51 ± 0.005	1.45 ± 0.01
$y_\mu/10^{-2}$	0.21 ± 0.002	1.08 ± 0.01	3.07 ± 0.03
$y_\tau/10^{-1}$	0.36 ± 0.003	1.89 ± 0.01	6.53 ± 0.06
$\lvert V_{us}\rvert/10^{-2}$	22.53 ± 0.07	22.53 ± 0.07	22.53 ± 0.07
$\lvert V_{cb}\rvert/10^{-2}$	3.72 ± 0.05	3.70 ± 0.05	3.37 ± 0.05
$\lvert V_{ub}\rvert/10^{-3}$	3.22 ± 0.11	3.21 ± 0.11	2.92 ± 0.10
η_W	0.35 ± 0.01	0.35 ± 0.01	0.35 ± 0.01

during the optimization. As before, for the charged leptons, we assume a relative 1% uncertainty in order to take into account the theoretical uncertainties such as SUSY and GUT scale threshold effects.

TABLE XI. Model parameters fixed by minimization for the flavor symmetry based models defined in Eqs. (2.43)–(2.45) by employing Monte Carlo analysis with different values of p.

p	2	1	0
$\tan\beta$	5	25	55
ϵ	0.1956 ± 0.0097	0.1985 ± 0.0105	0.1755 ± 0.0098

The numerical values of the model parameter determined by χ^2 minimization are presented in Table XI. These values are similar to the ones computed in Table II of Ref. [23]. The best fit values resulting from the χ^2 minimization for the three cases with $p = 0, 1, 2$ are presented in Table XII. From this table one sees that, for this class of models with a single parameter, the fit to the charged fermion observables is not very different from that of the models with three parameters. For V_{us}, the pull is greater than 2σ, but the rest of the observables are in good agreement. The main difference of this model compared to the previous two models is in the neutrino mixing parameters. In the $SU(5)$-based GUTs, the set of models where the left-handed light neutrino Yukawa coupling matrix elements are all $\sim O(1)$, large values of mixing angles are preferred for all three mixing parameters $\sin^2 2\theta_{ij}$ (see Fig. 3). On the other hand, the present model, which is described by the Yukawa matrices given in Eqs. (2.43)–(2.45), $O(1)$ entries exist only in the 2–3 sector that give rise to large $\sin^2 2\theta_{23}$. But due to a suppression factor ϵ in the 1–3 sector, $\sin^2 2\theta_{13}$

TABLE XII. χ^2 best fit values of the observables for the $SU(5)$-inspired flavor symmetry based models defined in Eqs. (2.43)–(2.45) with fixed values of the model parameters given in Table XI. The best fit values shown in this table correspond to $\chi^2/n_{obs} = 0.73$, 0.74, and 1.05 for $p = 2$, 1, and 0, respectively. Here TMV = theoretical mean value, TSD = theoretical standard deviation, ECV = experimental central value, and pull is defined in Eq. (3.2).

	TMV ± TSD			$\frac{\text{TMV}}{\text{ECV}}$			Pull		
Observables	$\tan\beta = 5$	$\tan\beta = 25$	$\tan\beta = 55$	$\tan\beta = 5$	$\tan\beta = 25$	$\tan\beta = 55$	$\tan\beta = 5$	$\tan\beta = 25$	$\tan\beta = 55$
$y_u/10^{-6}$	4.88 ± 5.61	5.42 ± 6.06	2.00 ± 2.26	1.63	1.88	0.67	0.33	0.41	−0.38
$y_c/10^{-3}$	2.42 ± 2.47	2.59 ± 2.66	1.62 ± 1.76	1.66	1.84	1.12	0.39	0.44	0.10
y_t	0.89 ± 0.46	0.89 ± 0.46	0.88 ± 0.46	1.64	1.70	1.51	0.76	0.79	0.64
$y_d/10^{-5}$	1.97 ± 1.39	11.0 ± 7.78	30.8 ± 22.6	0.80	0.88	0.86	−0.33	−0.18	−0.20
$y_s/10^{-3}$	1.37 ± 0.65	7.31 ± 3.49	28.4 ± 13.6	2.83	2.95	4.04	1.36	1.38	1.57
$y_b/10^{-1}$	0.51 ± 0.18	2.65 ± 0.94	13.4 ± 4.77	1.86	1.85	2.71	1.30	1.29	1.77
$y_e/10^{-5}$	1.96 ± 1.14	11.10 ± 7.88	31.06 ± 22.69	1.95	2.16	2.13	0.67	0.75	0.72
$y_\mu/10^{-3}$	1.36 ± 0.64	7.24 ± 3.45	28.42 ± 13.85	0.64	0.67	0.92	−1.16	−1.02	−0.16
$y_\tau/10^{-1}$	0.51 ± 0.18	2.66 ± 0.93	13.40 ± 4.75	1.43	1.40	2.05	0.85	0.82	1.44
$\lvert V_{us}\rvert/10^{-1}$	0.75 ± 0.72	0.77 ± 0.69	0.61 ± 0.59	0.33	0.34	0.27	−2.05	−2.11	−2.75
$\lvert V_{cb}\rvert/10^{-1}$	0.65 ± 0.62	0.66 ± 0.65	0.53 ± 0.54	1.74	1.79	1.57	0.44	0.45	0.35
$\lvert V_{ub}\rvert/10^{-2}$	0.31 ± 0.36	0.32 ± 0.36	0.20 ± 0.24	0.98	1.01	0.69	−0.01	0.01	−0.36
η_W	0.04 ± 5.56	0.01 ± 2.49	0.04 ± 2.72	0.11	0.02	0.11	−0.05	−0.13	−0.11
$\frac{\Delta m^2_{sol}}{\Delta m^2_{atm}}$	0.09 ± 0.16	0.10 ± 0.16	0.09 ± 0.16	3.17	3.27	3.21	0.42	0.43	0.41
$\sin^2\theta_{12}^{PMNS}$	0.17 ± 0.19	0.17 ± 0.19	0.15 ± 0.18	0.56	0.57	0.50	−0.70	−0.66	−0.84
$\sin^2\theta_{23}^{PMNS}$	0.47 ± 0.29	0.47 ± 0.29	0.48 ± 0.29	1.22	1.24	1.22	0.31	0.30	0.30
$\sin^2\theta_{13}^{PMNS}$	0.09 ± 0.12	0.10 ± 0.12	0.08 ± 0.11	3.97	4.14	3.44	0.57	0.58	0.51

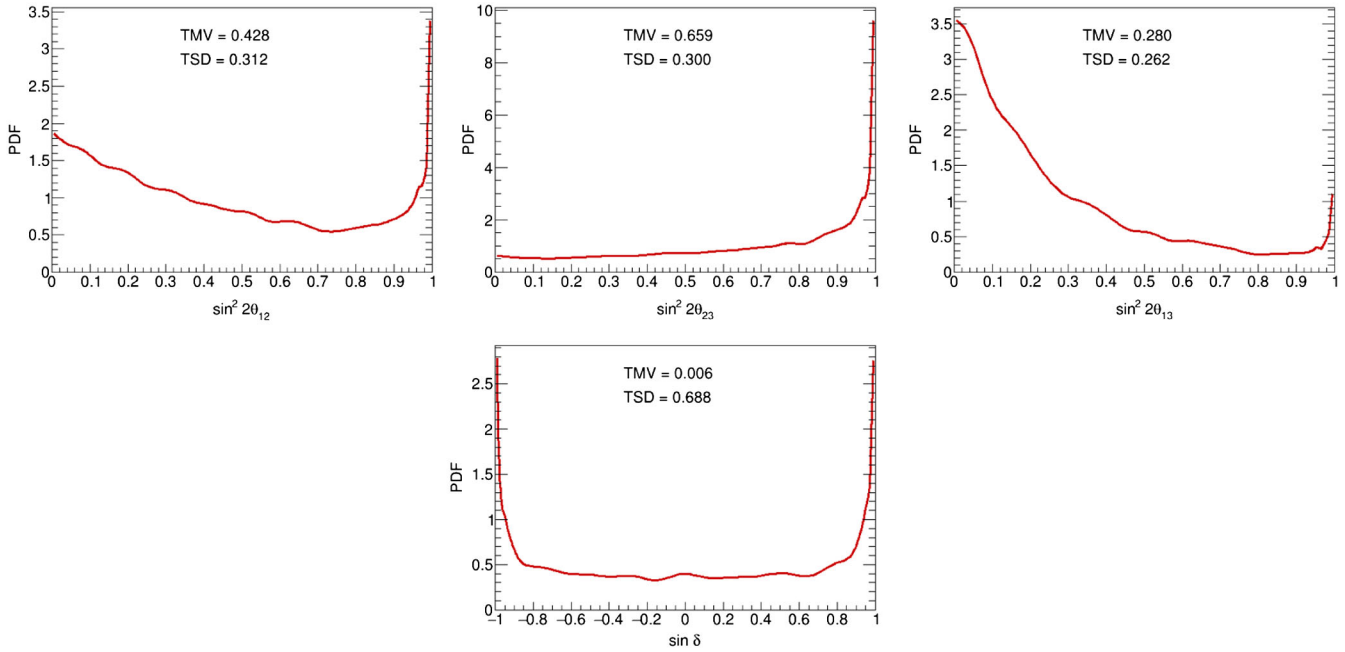

FIG. 5. Probability density plots for the neutrino mixing parameters for the $SU(5)$-inspired flavor symmetry based models defined in Eqs. (2.43)–(2.45). The upper plots are for the mixing angles, $\sin^2 2\theta_{ij}$, and the lower plot is for CP-violating parameter $\sin\delta$.

naturally comes out to be smaller than unity. The probability density plots of $\sin^2 2\theta_{ij}$ are shown in Fig. 5, and the patterns remain the same for different values of p for this set of models (Fig. 6) compared to the previous set analyzed before (Fig. 4). Except for the three mixing parameters, the theoretical distributions of the observables in the fermion sector remain similar in pattern and are shown in Fig. 9 in Appendix A 2 for the case of $p = 2$

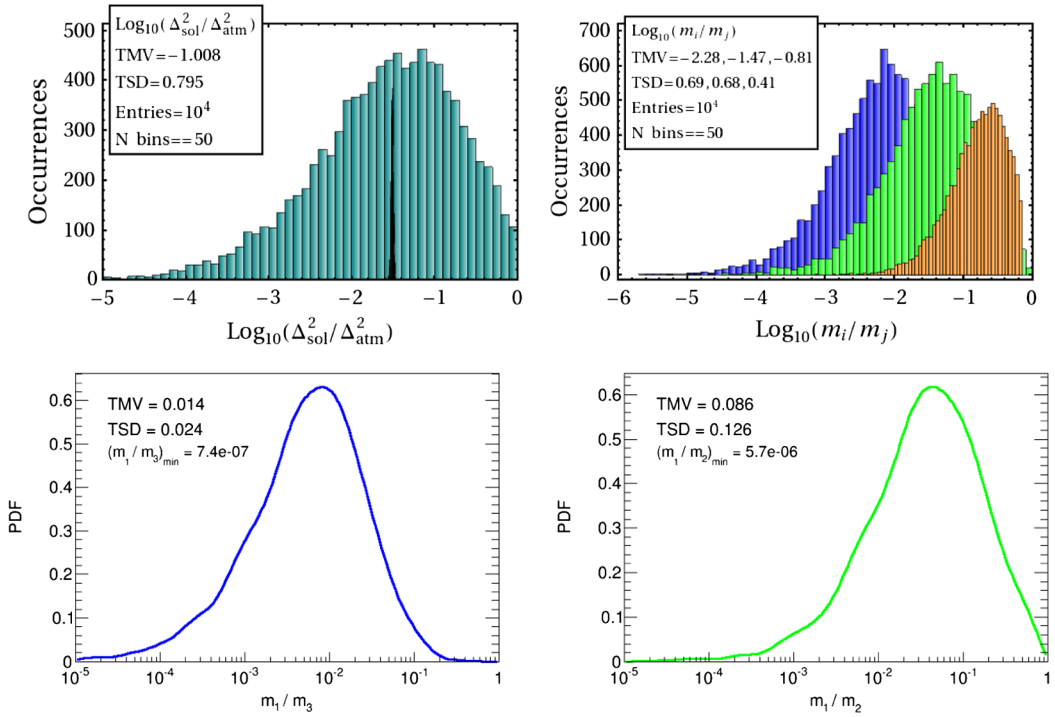

FIG. 6. The theoretical distributions and the probability density plots of the observables in the neutrino sector for the $SU(5)$-inspired flavor symmetry based models defined in Eqs. (2.43)–(2.45). The notation is the same as in Fig. 4.

(histograms for other values of p's are similar, and are not shown).

IV. A VARIANT MONTE CARLO ANALYSIS OF THE $SU(5)$-BASED MODELS

The Monte Carlo analysis of Sec. III treats the random variables as an unbiased set with Gaussian distribution and investigates the likelihood of these models to procreate the experimental values. The results presented in the previous section show that, on average, the agreement of the theoretical mean values with the experimental central values is very good, except for a few observables for which the theoretical mean values do not coincide with the experimental central values, but still the experimental central values lie within the range of values predicted by the theory. Since we have no control over the random variables, the theoretical standard deviations of each observables are quite large (as can be seen from columns 4 and 5 of Table VI) and of the same order as the theoretical mean values. In this section, we present a modified version of the Monte Carlo analysis, where the model parameters, ϵ_i, are not fixed but rather treated as constrained random parameters. As before, we start with the set of uncorrelated random variables having Gaussian distribution and analyze the class of models with Yukawa coupling matrices given by Eqs. (2.1)–(2.5). We consider a projection of these distributions onto a subspace of the original space of random parameters defined by the experimental constraints. These constraints create correlations between the random parameters, and therefore their distributions in the constrained subspace are in general different from the original (unconstrained) distributions. We optimize the model parameters by minimizing the difference between the complete set $\{\boldsymbol{r}\}$ of random parameters describing a given class of models, and the subset $\{\boldsymbol{r}^*\}$ of random parameters describing the models that satisfy the experimental constraints $O_{i\mathrm{th}} = E_{i\,\mathrm{exp}}$, which we call the distortion and denote by $D(\{\boldsymbol{r}^*\},\{\boldsymbol{r}\})$. The condition of optimization is then

$$\boldsymbol{\epsilon}_{\mathrm{best}} = \mathrm{argmin}_{\boldsymbol{\epsilon}} D(\{\boldsymbol{r}^*\},\{\boldsymbol{r}\}). \tag{4.1}$$

To implement the optimization procedure, we modify the χ^2 minimization approach described in the previous sections by introducing an additional step which, starting from the initial set of random parameters $\{\boldsymbol{r}_0\}$, tries to update the current set of random parameters $\{\boldsymbol{r}\}$ by minimizing $D = D(O,E) + D(\{\boldsymbol{r}\},\{\boldsymbol{r}_0\})$, where

$$D(O,E) = \sum \left(\frac{O_{i\mathrm{th}} - E_{i\,\mathrm{exp}}}{\sigma_{i\,\mathrm{exp}}}\right)^2 \tag{4.2}$$

TABLE XIII. Best fit values of the observables for the $SU(5)$-based GUTs defined in Eqs. (2.1)–(2.5) by employing the modified Monte Carlo analysis. Here we have considered the case with $\tan\beta = 10$ as input. As explained in the text, these results correspond to minimization of the function $D = D(O,E) + D(\{\boldsymbol{r}^*\},\{\boldsymbol{r}\})$. This fit corresponds to $D(O,E)/n_{\mathrm{obs}} = 0.03$. Here TMV = theoretical mean value, TSD = theoretical standard deviation, ECV = experimental central value, and pull is defined in Eq. (3.2).

Observables	TMV ± TSD	$\frac{\mathrm{TMV}}{\mathrm{ECV}}$	Pull
$y_u/10^{-6}$	2.57 ± 0.09	1.00	0.00
$y_c/10^{-3}$	1.40 ± 0.03	1.02	0.39
y_t	0.545 ± 0.053	1.02	0.25
$y_d/10^{-4}$	0.39 ± 0.04	0.99	−0.05
$y_s/10^{-3}$	0.75 ± 0.03	1.02	0.28
$y_b/10^{-2}$	4.49 ± 0.22	0.99	−0.02
$y_e/10^{-5}$	1.64 ± 0.001	1.00	0.18
$y_\mu/10^{-3}$	3.46 ± 0.002	1.00	0.11
$y_\tau/10^{-1}$	0.589 ± 0.001	0.99	−0.09
$\lvert V_{us}\rvert$	0.225 ± 0.0009	0.99	−0.29
$\lvert V_{cb}\rvert/10^{-2}$	3.75 ± 0.017	1.00	0.04
$\lvert V_{ub}\rvert/10^{-3}$	3.24 ± 0.03	0.99	−0.01
η_W	0.35 ± 0.004	1.00	0.00

accounts for discrepancy between the model prediction and experiment, and the measure of distortion is chosen to be

$$D(\{\boldsymbol{r}\},\{\boldsymbol{r}_0\}) = \sum \frac{(C_{jk} - \mathbf{E}[C_{jk}])^2}{\mathbf{E}[C_{jk}]}, \tag{4.3}$$

where C_{jk} is the number of occurrences of the binned value of the expected cumulative distribution function (cdf) of random variable r_j, and the sum is taken over all cdf bins k and all elements of all random matrices j in the model. The method we use is an iterative procedure that alternates the χ^2 minimization and $\{\boldsymbol{r}\}$ optimization steps. The best fit results of this procedure obtained for the $SU(5)$-based GUTs defined in Eqs. (2.1)–(2.5) are presented in Table XIII. Here we have considered the case with $\tan\beta = 10$ as input. The model parameters that are extracted from this procedure are given in Eq. (4.4),

$$\begin{aligned} \varepsilon_1 &= 0.00106 \pm 0.00001, \\ \varepsilon_2 &= 0.08023 \pm 0.00044, \\ \varepsilon_4 &= 0.03294 \pm 0.00024. \end{aligned} \tag{4.4}$$

The best fit values presented in Table XIII correspond to $D(O,E) = 0.43$. In this modified approach, all the theoretically predicted values of the observables almost coincide with the experimental measured values. Compared to the approach explained in the previous

TABLE XIV. Best fit values of observables using the modified approach of Monte Carlo analysis in the neutrino sector for $SU(5)$-based GUTs defined in Eqs. (2.1)–(2.5). The best fit values shown in this table correspond to $\chi^2/n_{\rm obs} = 0.1$. Here TMV = theoretical mean value, TSD = theoretical standard deviation, ECV = experimental central value, and pull is defined in Eq. (3.2).

Observables	TMV ± TSD	$\frac{\rm TMV}{\rm ECV}$	Pull
$\frac{\Delta m^2_{\rm sol}}{\Delta m^2_{\rm atm}}$	0.031 ± 0.0002	1.0	0.01
$\sin^2\theta_{12}$	0.31 ± 0.02	0.99	0.17
$\sin^2\theta_{23}$	0.39 ± 0.03	0.99	0.23
$\sin^2\theta_{13}$	0.024 ± 0.001	1.0	0.12

sections, theoretical errors are greatly reduced and comparable to the experimental uncertainties. Histogram distributions of the observables in the charged fermion sector corresponding to this result are presented in Fig. 10 in Appendix B 1, and the distributions of the restricted set $\{r^*\}$ are shown in Figs. 11, 12, and 13 in Appendix B 2 for the matrices Y^0_U, Y^0_D, and Y^0_L, respectively. We also employ this approach in the neutrino sector Eq. (2.7) separately,

TABLE XV. Comparison of probabilities of the two unmeasured quantities in the neutrino sector for the $SU(5)$-based GUTs with different neutrino mass matrix structures. For the quantity $\sin\delta$, these probabilities in the negative side remain roughly the same in the separate domains as for the positive side. Square brackets represent the end points that are included in the set, whereas for the round brackets the end points are not included.

Quantity		Structureless neutrino matrix	Hierarchical neutrino matrix
m_1/m_2	≤ 0.01	4.24%	20.38%
	≤ 0.1	33.77%	74.57%
	≤ 0.2	56.23%	88.33%
$\sin\delta$	[0,0.25]	8.15%	8.9%
	(0.25,0.5]	8.79%	9.82%
	(0.5,0.75]	9.68%	10.16%
	(0.75,1.0]	23.87%	21.18%

where the model parameters ϵ_i are absent. The results that correspond to $D(O,E) = 0.1$ are presented in Table XIV. The histogram distributions of the theoretical predictions of these quantities in the neutrino sector are shown in Fig. 14 in Appendix B 3 and the modified set $\{r^*\}$ in

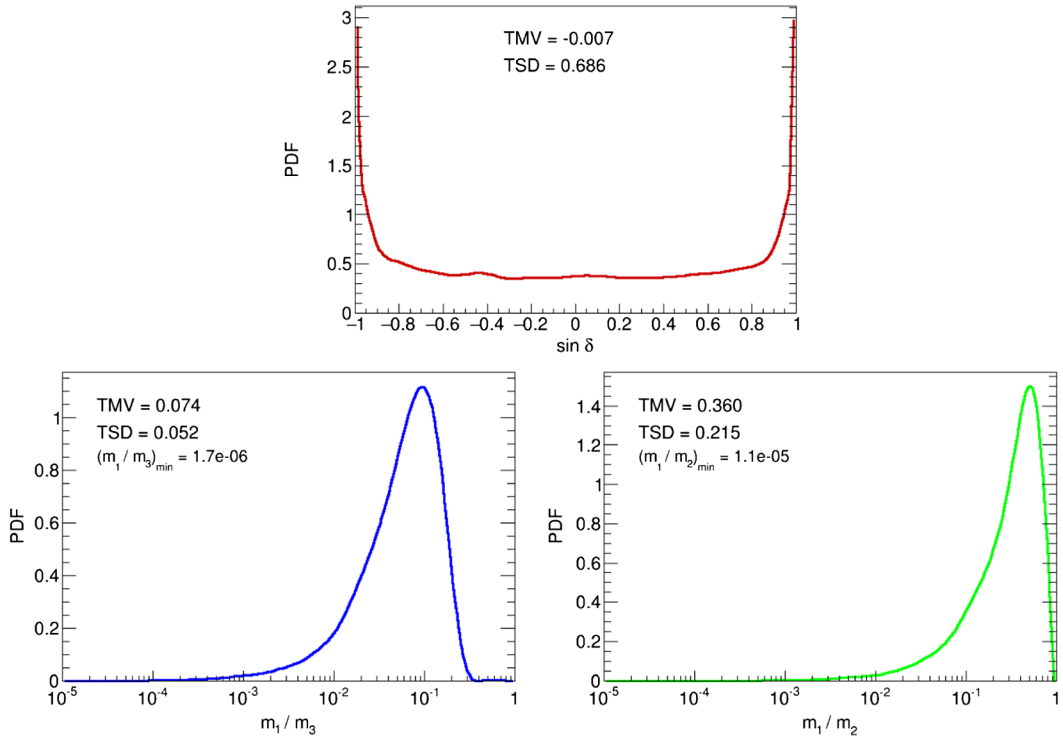

FIG. 7. Probability density plots of the experimentally unmeasured quantities in the neutrino sector, the sine of the Dirac-type phase (upper) and neutrino mass ratios m_1/m_3 (lower left) and m_1/m_2 (lower right) by employing the modified Monte Carlo analysis for $SU(5)$-based GUTs defined in Eqs. (2.1)–(2.5).

Figs. 15 and 16 in Appendix B 4. The $\sin\delta$ and the two neutrino mass ratios m_1/m_3 and m_1/m_2 are shown in Fig. 7. This variant of the Monte Carlo analysis shows that with the subspace $\{\boldsymbol{r}^*\}$ which does not have much deviation from the original landscape $\boldsymbol{r}$, excellent agreement of the observables to the experimental measured values can be achieved. One can in principle apply this modified approach to the special cases of the $SU(5)$-based GUTs explained in Sec. II B but we do not include those analysis here.

V. CONCLUSION

In this paper we have extended the idea of anarchy from the neutrino sector to the quark and charged lepton sectors. This is made possible in the context of $SU(5)$ unified theories where the 10_i fermions mix with vectorlike $10_\alpha + \overline{10}_\alpha$ fermions having GUT scale masses. While all the Yukawa couplings in these models are of order one, these mixings provide three hierarchical parameters which explain all the hierarchies in the charged fermion masses and quark mixing angles. The neutrino sector is immune to such mixings and remains anarchical. We have also studied special cases of this general $SU(5)$ setup with a smaller number of input parameters—either 2 or 1—by introducing a flavor $U(1)$ symmetry that distinguishes the three families of 10_i fermions.

We have presented detailed quantitative analysis of these models following a probabilistic approach. The Yukawa couplings of the model are assumed to be uncorrelated random variables obeying Gaussian distributions. Our Monte Carlo analysis shows that the combined anarchy-hierarchy scenario gives a very good fit to all the fermion masses and mixings. We have also presented a variant Monte Carlo method where the model parameters are not kept fixed but have certain distributions constrained by the phenomenological considerations. This approach is proposed to systematically explore the subspace of the original Gaussian landscape that becomes consistent with all experimental constraints with greater accuracy. A figure of merit in this approach is the distortion of the distributions compared to the original Gaussian distributions. The framework is found to provide a good quality fit.

The theoretical distributions of the observables in the charged fermion sector remain roughly the same for the various models studied here. There is one important difference in the neutrino mixing parameters in the flavor $U(1)$ model that distinguishes the $\bar{5}_1$ from $\bar{5}_{2,3}$ fields: The mixing parameter $\sin\theta_{13}$ comes out to be somewhat smaller than $\sin\theta_{23}$. Anarchy prefers normal ordering of the neutrino mass spectrum with a mild hierarchy in the masses. A comparison of the two experimentally unmeasured quantities in the neutrino sector, the mass ratio m_1/m_2, and the CP-violating parameter $\sin\delta$ predicted by our statistical analysis for the two different sets of models studied here is presented in Table XV.

ACKNOWLEDGMENTS

K. S. B. and S. S. would like to thank the organizers of CETUP* 2015 for hospitality and partial support during the 2015 Summer Program at Lead, South Dakota, where part of the work was done. They would also like to thank the participants of CETUP* 2015 for helpful discussions and comments. This work has been supported in part by the U.S. Department of Energy Grant No. de-sc0016013. Part of the numerical calculations was performed using the High Performance Computing Center at Oklahoma State University (NSF Grant No. OCI-1126330).

APPENDIX A: DISTRIBUTIONS OF THE OBSERVABLES IN THE CHARGED FERMION SECTOR FOR THE $SU(5)$-INSPIRED $U(1)$ FLAVOR MODELS

1. Models with two parameters

Here we present the theoretical distributions of the observables in the charged fermion sector for the $SU(5)$-inspired $U(1)$ flavor symmetry models with the charge assignment $\{q_1 = 1, q_2 = 0, p = 0\}$ defined by Eqs. (2.1)–(2.5) and (2.42) and with two parameters $\{\epsilon, \epsilon_4\}$. These are shown in Fig. 8.

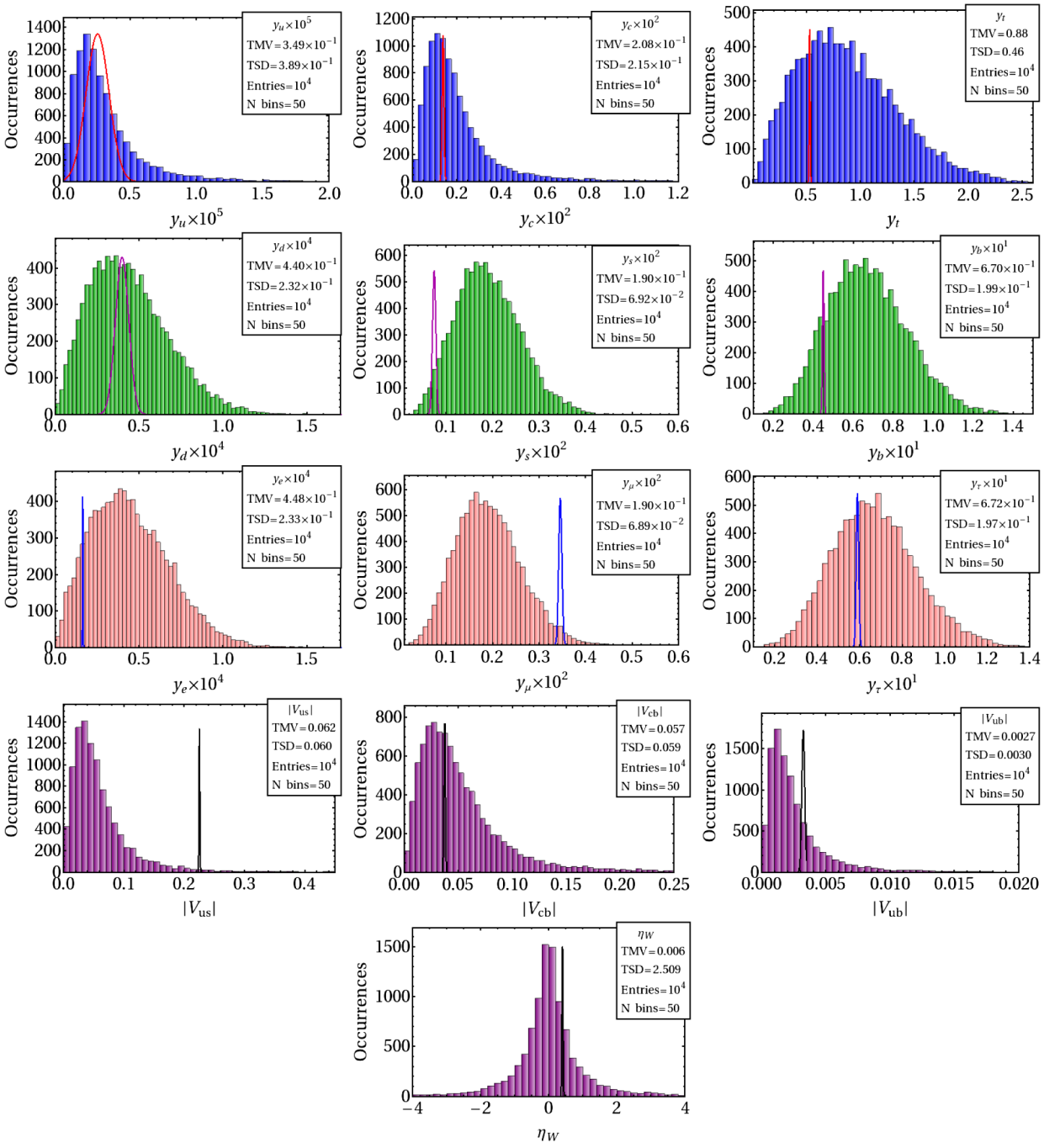

FIG. 8. Histograms showing the theoretical distributions of the observables in the charged fermion sector in the $SU(5)$-inspired $U(1)$ flavor symmetric models with the charge assignment $\{q_1 = 1, q_2 = 0, p = 0\}$ defined by Eqs. (2.1)–(2.5) and (2.42) ($\tan\beta = 10$). The color code is the same as in Fig. 1.

2. Models with single parameter

Here we present the theoretical distributions of the observables in the charged fermion sector for the $SU(5)$-inspired $U(1)$ flavor symmetry models with the charge assignment $\{q_1 = 2, q_2 = 1, p = 2\}$ defined by Eqs. (2.43)–(2.45) and with a single parameter $\{\epsilon\}$. The results are shown in Fig. 9.

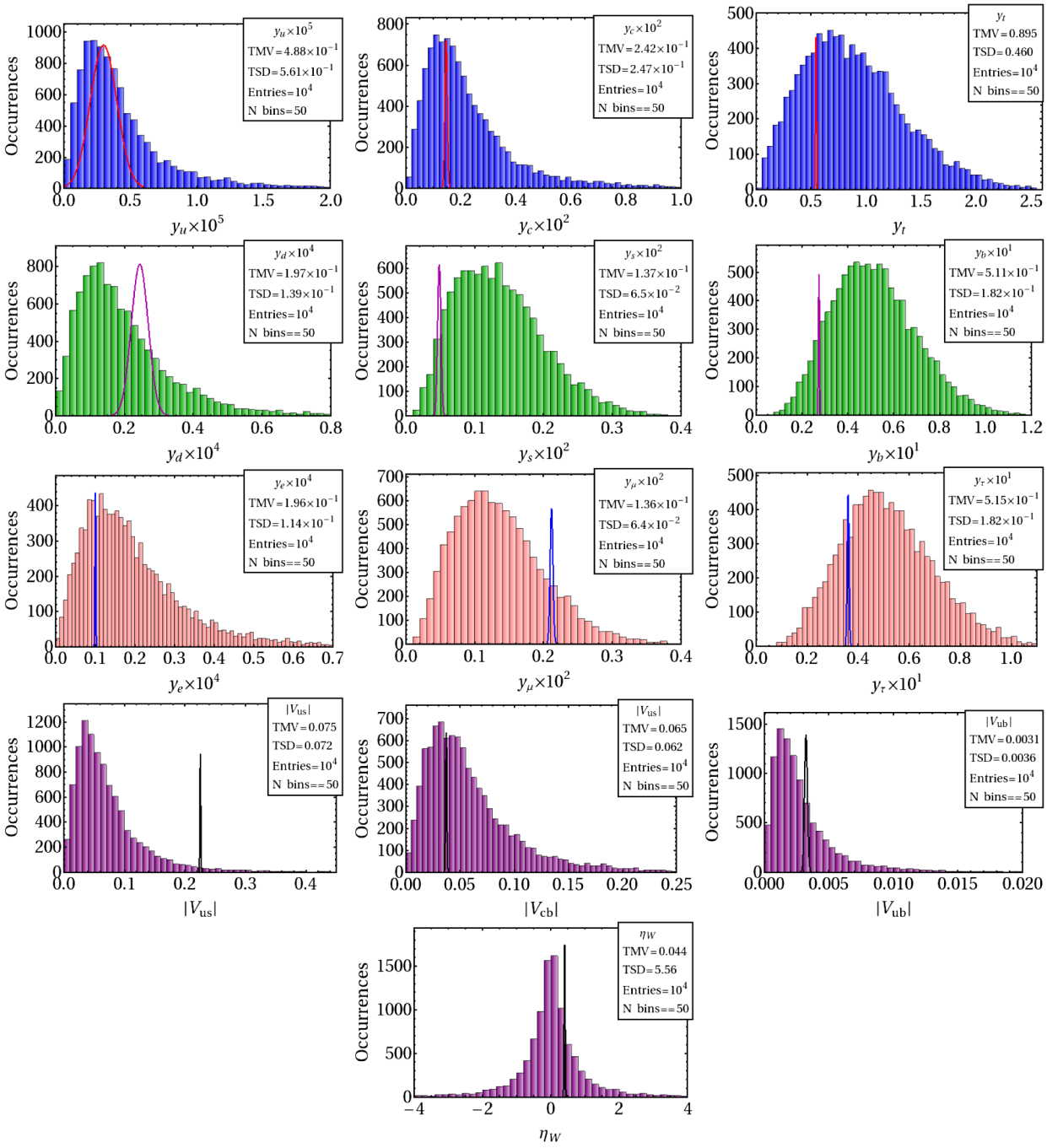

FIG. 9. Histograms showing the theoretical distributions of the observables in the charged fermion sector according to the $SU(5)$-inspired $U(1)$ flavor symmetry based models with the charge assignment $\{q_1 = 2, q_2 = 1, p = 2\}$ defined by Eqs. (2.43)–(2.45) ($\tan\beta = 5$). The color code is the same as in Fig. 1.

APPENDIX B: DISTRIBUTIONS OF THE OBSERVABLES AND RANDOM ENTRIES RESULTING FROM THE MODIFIED MONTE CARLO ANALYSIS

1. Distributions of the observables resulting from the subset obtained by the modified Monte Carlo analysis in the charged fermion sector

Here we present the distributions of the observables in Fig. 10 in the charged fermion sector that resulted from the $D = D(O, E) + D(\{\boldsymbol{r}^*\}, \{\boldsymbol{r}\})$ minimization procedure following the modified Monte Carlo analysis as explained in Sec. IV

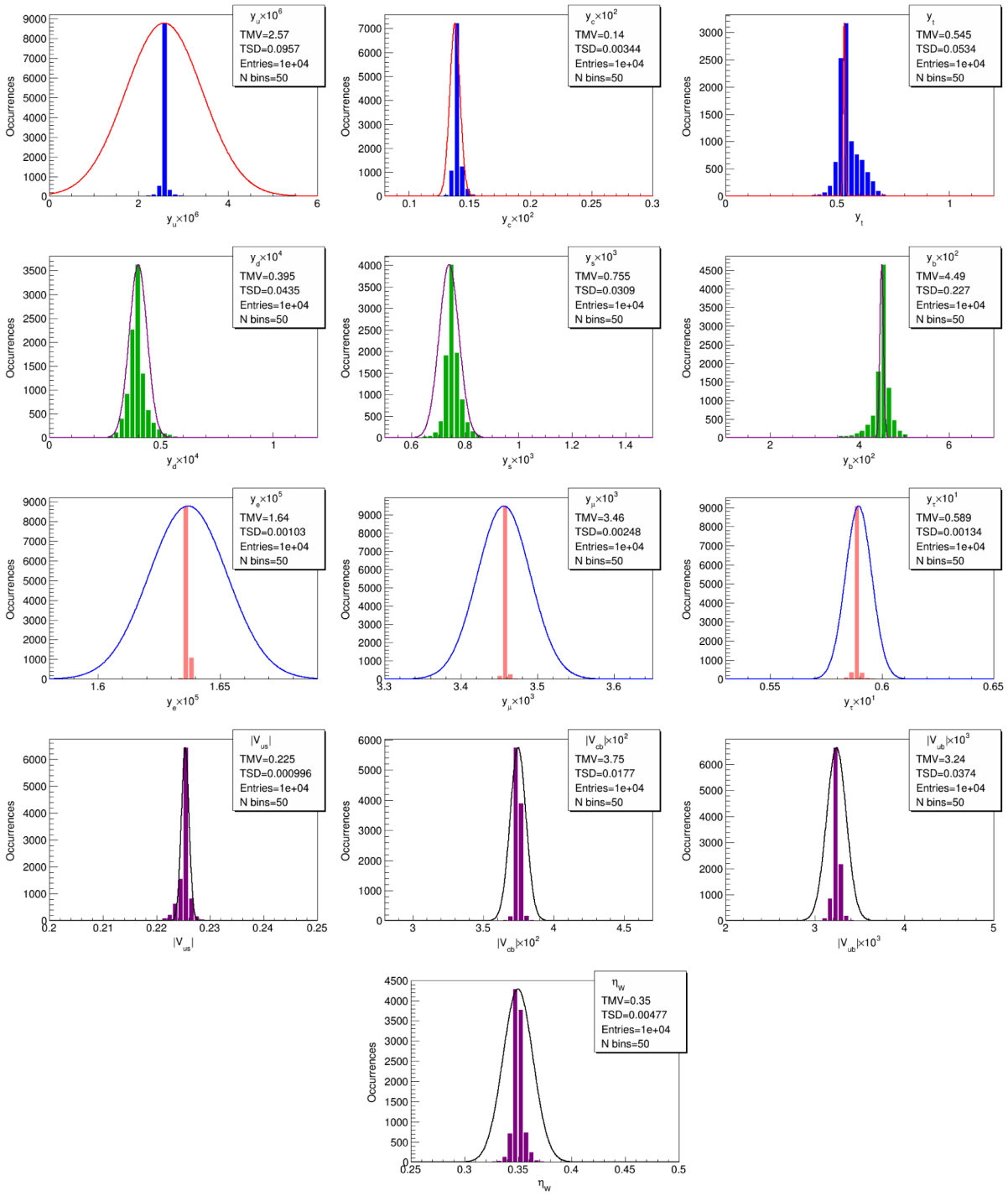

FIG. 10. Histogram distributions of the observables in the charged fermion sector according to the modified Monte Carlo method for $SU(5)$-based GUTs defined in Eqs. (2.1)–(2.5) with $\tan\beta = 10$. Color code is the same as Fig. 1. Note the change of scales compared to Fig. 1 for A few of the plots ($y_u \times 10^5 \to y_u \times 10^6$, $y_s \times 10^2 \to y_s \times 10^3$, $y_e \times 10^4 \to y_e \times 10^5$, $y_\mu \times 10^2 \to y_\mu \times 10^3$, $|V_{cb}| \to |V_{cb}| \times 10^2$, $|V_{ub}| \to |V_{ub}| \times 10^3$).

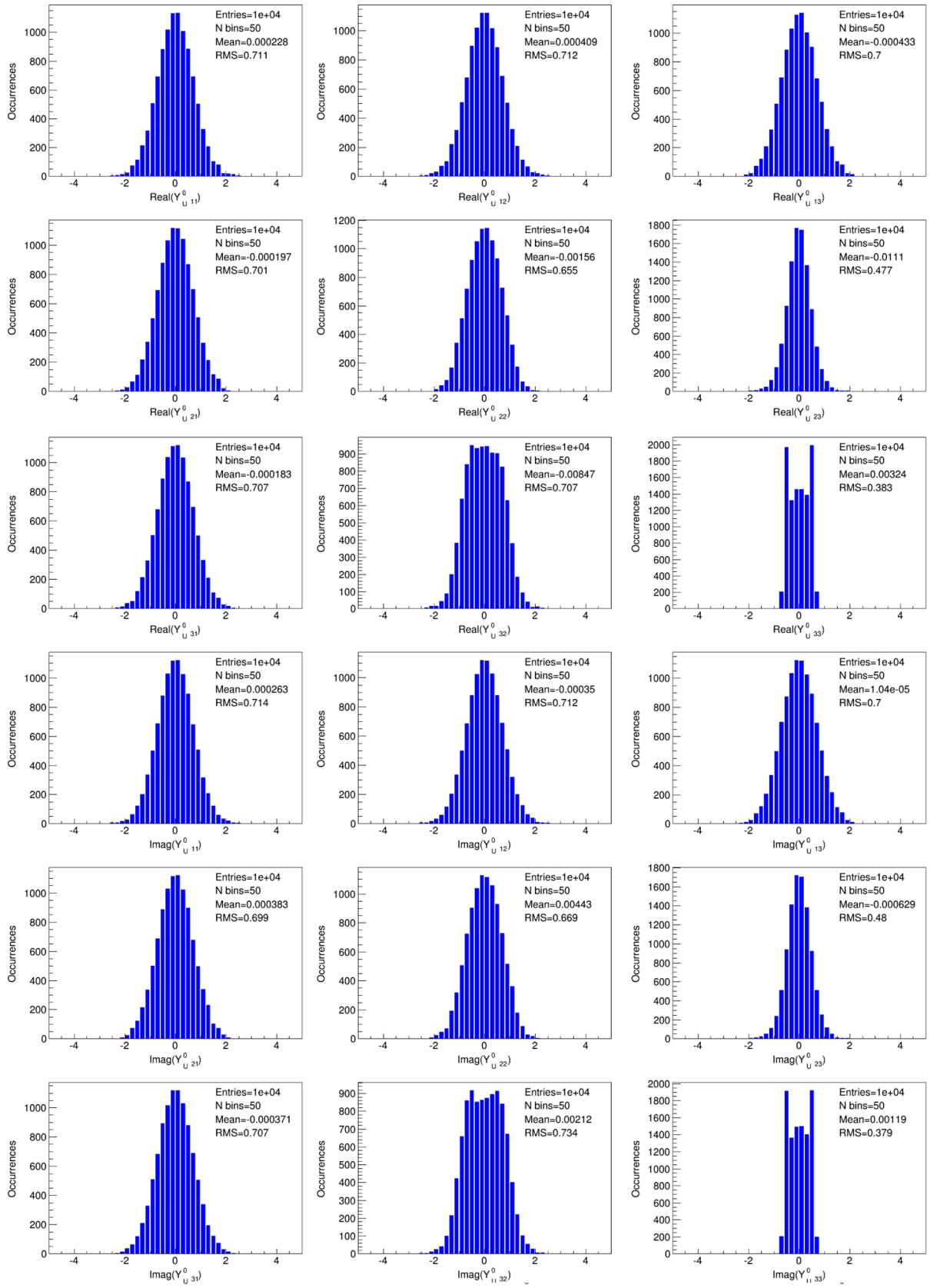

FIG. 11. Distributions of the $O(1)$ random entries in the matrix Y^0_U from the modified Monte Carlo analysis that produce the observables in Fig. 10 for $\tan\beta = 10$. The first nine of the plots are for the real parts and the next nine for imaginary parts of the matrix, Y^0_U. For all these plots sample size and number of bins are taken to be 10^4 and 50, respectively.

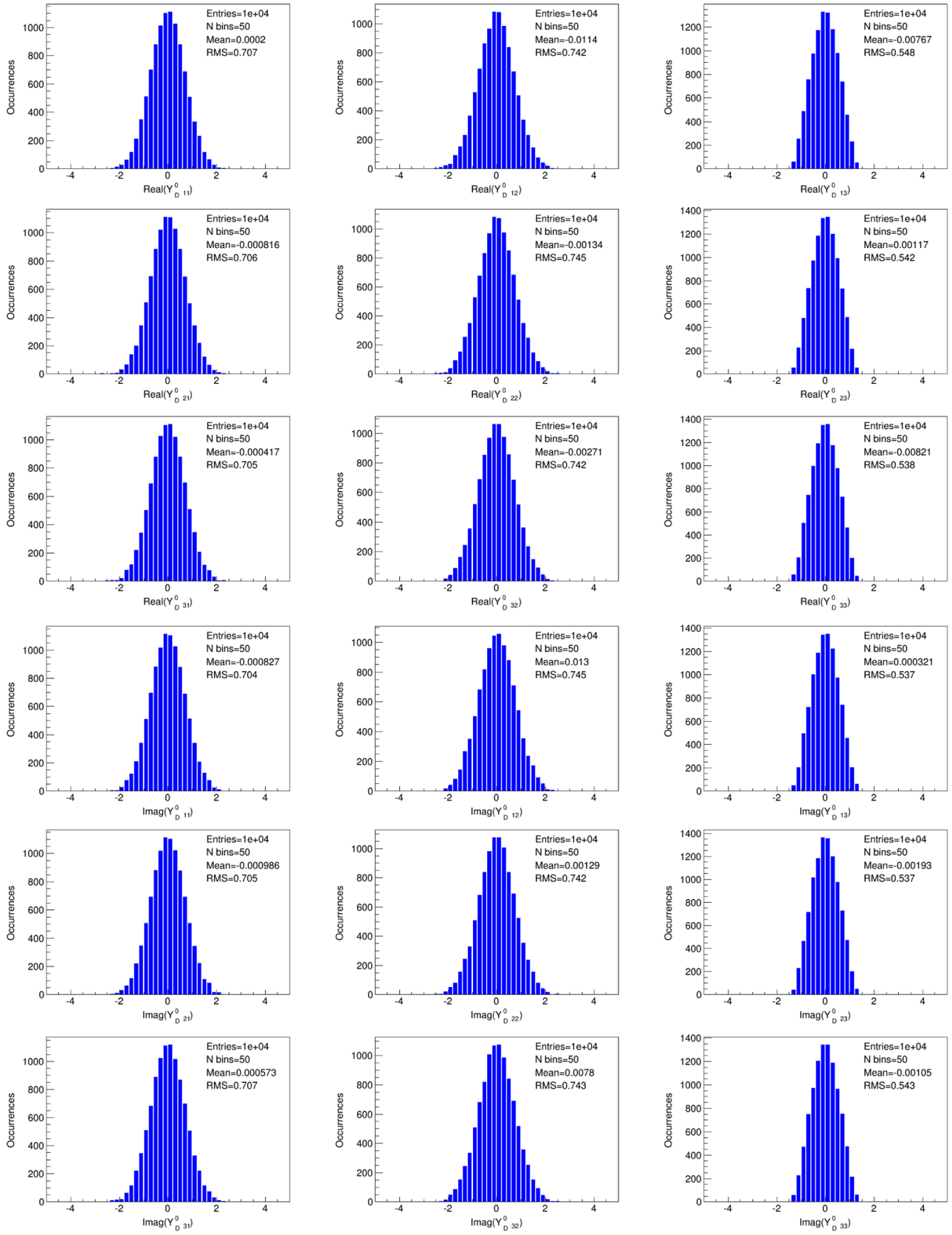

FIG. 12. Distributions of the $O(1)$ random entries in the matrix Y_D^0 from the modified Monte Carlo analysis that produce the observables in Fig. 10 for $\tan\beta = 10$. The first nine of the plots are for the real parts and the next nine for imaginary parts of the matrix, Y_D^0. For all these plots sample size and number of bins are taken to be 10^4 and 50, respectively.

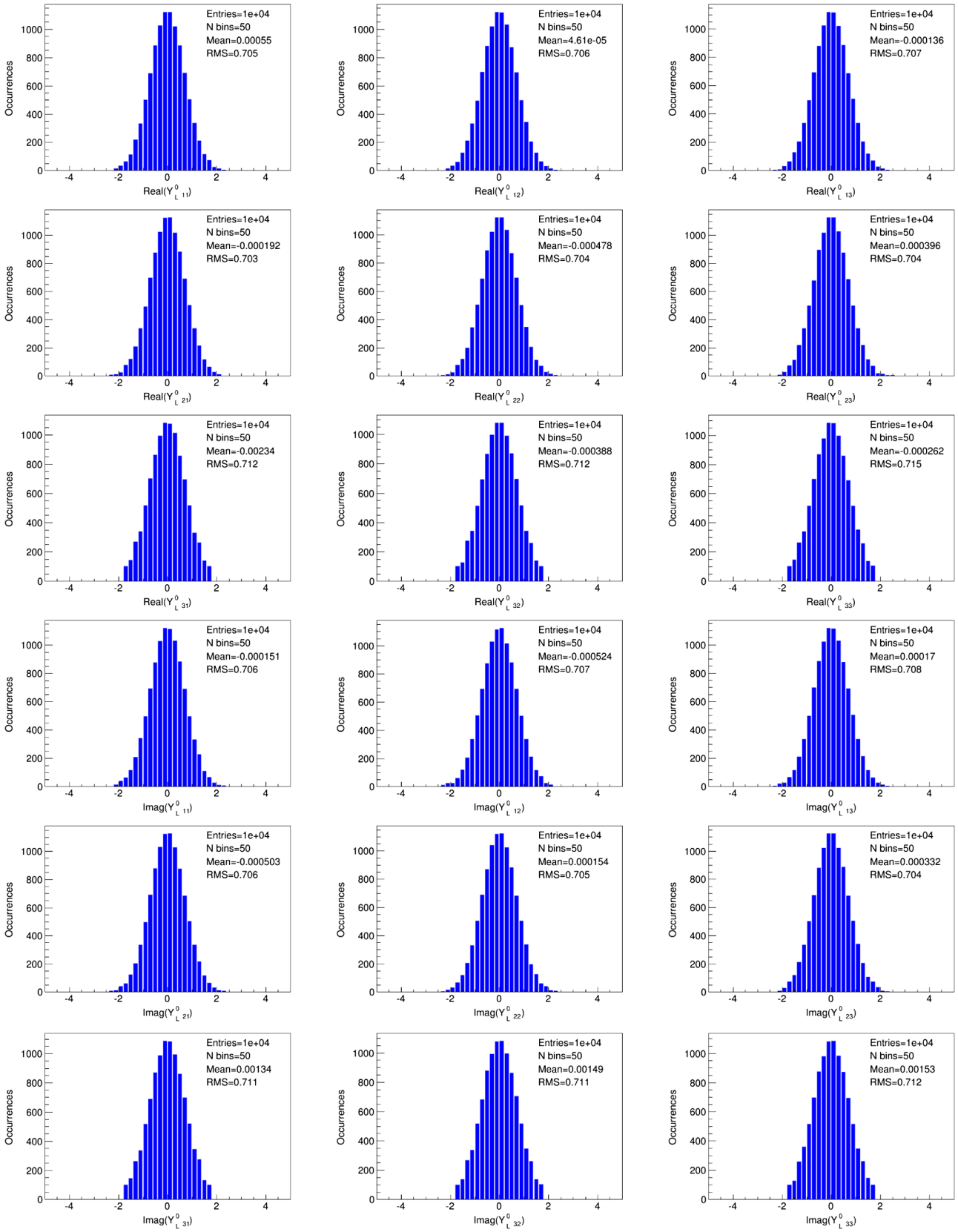

FIG. 13. Distributions of the $O(1)$ random entries in the matrix Y_L^0 from the modified Monte Carlo analysis that produce the observables in Fig. 10 for $\tan\beta = 10$. The first nine of the plots are for the real parts and the next nine for imaginary parts of the matrix, Y_L^0. For all these plots sample size and number of bins are taken to be 10^4 and 50, respectively.

for the $SU(5)$-based GUTs defined in Eqs. (2.1)–(2.5). The histogram plots of the observables in Fig. 10 show excellent agreement with the observation. All these quantities are reproduced roughly within their 1σ range even though the random matrices remain mostly random with only slight distortions.

2. Distributions of the projected random entries resulting from the modified Monte Carlo analysis in the charged fermion sector

Here we present the distributions of the modified random entries in Fig. 11 for up-quark, Fig. 12 for down-quark, and Fig. 13 for charged lepton matrices. These are the result of the $D = D(O, E) + D(\{\boldsymbol{r}^*\}, \{\boldsymbol{r}\})$ minimization procedure following the modified Monte Carlo analysis as explained in Sec. IV for the $SU(5)$-based GUTs defined in Eqs. (2.1)–(2.5). From Figs. 11, 12, and 13 one can see that the majority of the random entries of the matrices, even after the minimization process exhibit Gaussianity and remain similar in distribution as the unbiased set. The (3,3) element in the up-type quark Yukawa matrix is the only entry that shows somewhat distorted distribution. This analysis shows that the subspace of the random variables that has excellent agreement with experimental data is quite broad.

3. Distributions of the neutrino observables by applying the modified Monte Carlo analysis

Here we present the theoretical distributions of the neutrino observables in Fig. 14 by employing the modified Monte Carlo analysis for the $SU(5)$-based GUTs where the neutrino matrix if given by Eq. (2.7).

4. Distributions of the modified random entries in the neutrino sector by applying the modified Monte Carlo analysis

Here we present the distributions of the biased random entries in the neutrino sector. These random entries are the result by employing the modified Monte Carlo analysis. Modified random entries in the Dirac Yukawa coupling matrix are presented in Fig. 15 and in Fig. 16 for the entries in the right-handed Yukawa couplings. All these entries get barely modified from the unbiased pattern.

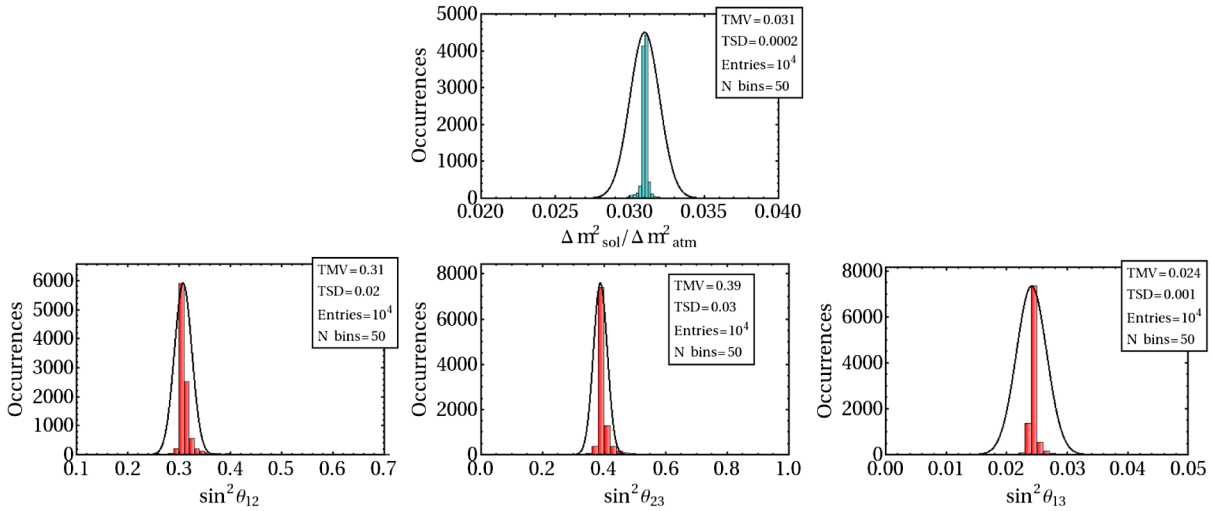

FIG. 14. Histogram distributions of the observables in the neutrino sector according to the modified Monte Carlo approach for $SU(5)$-based GUTs with a structureless neutrino mass matrix. The top histogram plot (dark cyan) shows the theoretical distribution of the quantity $\Delta m^2_{\rm sol}/\Delta m^2_{\rm atm}$, and the bottom three plots (red) are for the mixing parameters $\sin^2\theta_{ij}$. The black curves represent the experimental 1σ ranges. The sample size is taken to be 10^4, and the number of bins is taken to be 50.

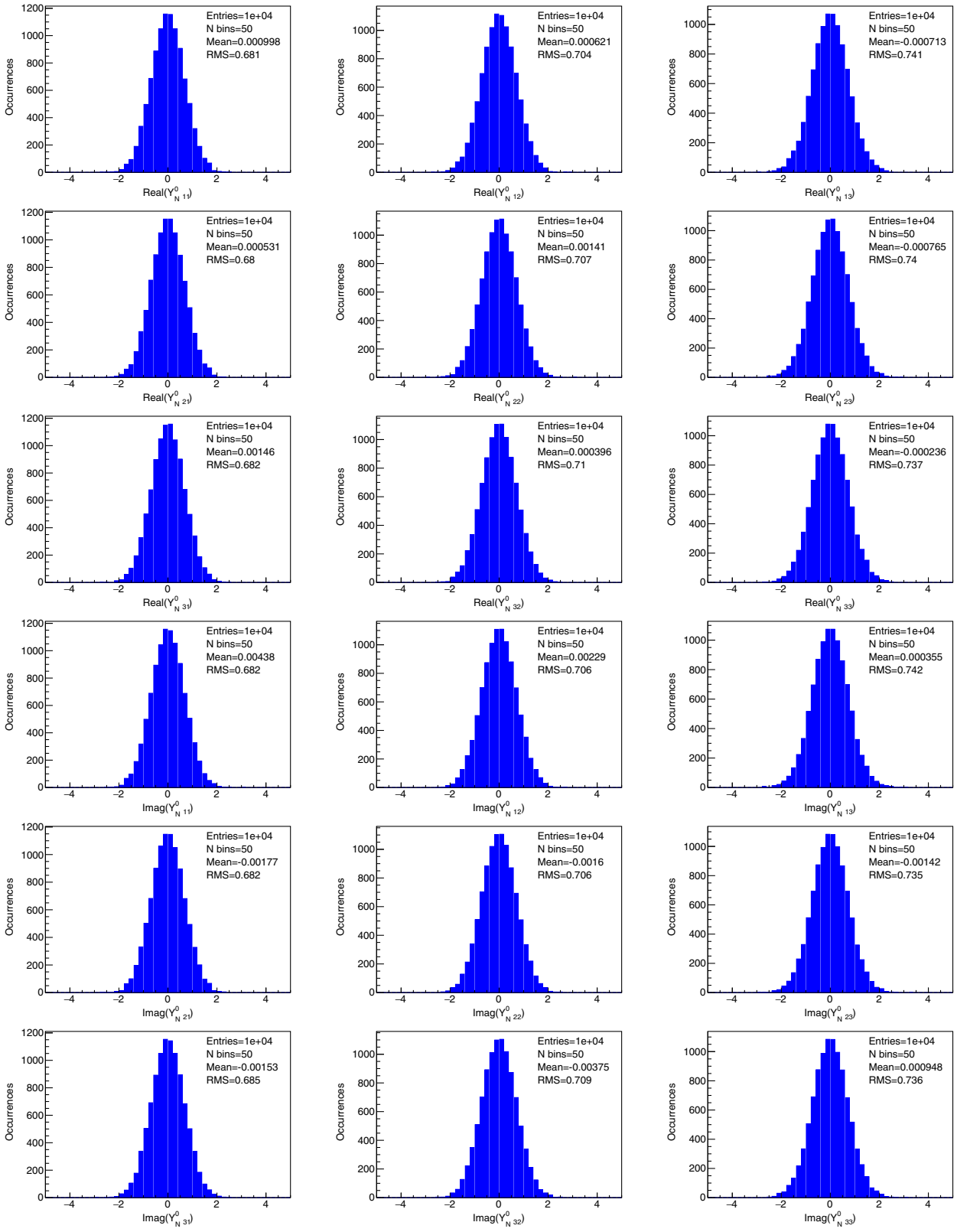

FIG. 15. Distributions of the $O(1)$ random entries in the matrix Y^0_N from the modified Monte Carlo approach that produce the observables in Fig. 14.

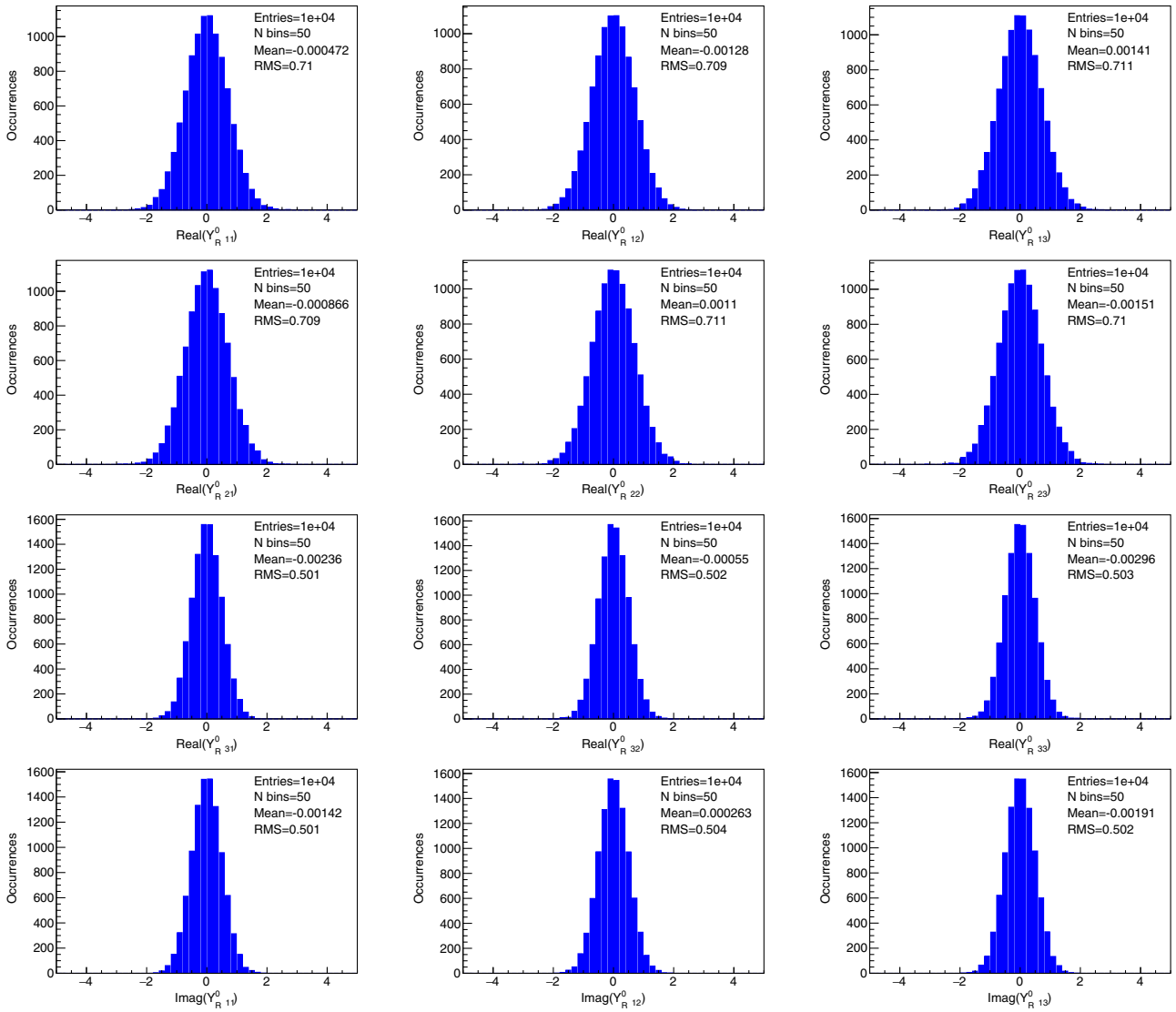

FIG. 16. Distributions of the $O(1)$ random entries in the matrix Y^0_R from the modified Monte Carlo approach that produces the observables in Fig. 14.

[1] Y. Fukuda *et al.* (Super-Kamiokande Collaboration), Evidence for Oscillation of Atmospheric Neutrinos, Phys. Rev. Lett. **81**, 1562 (1998).

[2] Q. R. Ahmad *et al.* (SNO Collaboration), Direct Evidence for Neutrino Flavor Transformation from Neutral Current Interactions in the Sudbury Neutrino Observatory, Phys. Rev. Lett. **89**, 011301 (2002).

[3] K. Abe *et al.* (T2K Collaboration), Indication of Electron Neutrino Appearance from an Accelerator-produced Off-Axis Muon Neutrino Beam, Phys. Rev. Lett. **107**, 041801 (2011); P. Adamson *et al.* (MINOS Collaboration), Improved Search for Muon-Neutrino to Electron-Neutrino Oscillations in MINOS, Phys. Rev. Lett. **107**, 181802 (2011).

[4] Y. Abe *et al.* (Double Chooz Collaboration), Indication for the Disappearance of Reactor Electron Antineutrinos in the Double Chooz Experiment, Phys. Rev. Lett. **108**, 131801 (2012); F. P. An *et al.* (Daya Bay Collaboration), Observation of Electron-Antineutrino Disappearance at Daya Bay, Phys. Rev. Lett. **108**, 171803 (2012); J. K.

Ahn *et al.* (RENO Collaboration), Observation of Reactor Electron Antineutrino Disappearance in the RENO Experiment, Phys. Rev. Lett. **108**, 191802 (2012).
[5] C. Patrignani *et al.* (Particle Data Group), Review of particle physics, Chin. Phys. C **40**, 100001 (2016).
[6] K. S. Babu, TASI lectures on flavor physics, arXiv: 0910.2948.
[7] L. J. Hall, H. Murayama, and N. Weiner, Neutrino Mass Anarchy, Phys. Rev. Lett. **84**, 2572 (2000).
[8] N. Haba and H. Murayama, Anarchy and hierarchy, Phys. Rev. D **63**, 053010 (2001).
[9] G. Altarelli, F. Feruglio, and I. Masina, Models of neutrino masses: Anarchy versus hierarchy, J. High Energy Phys. 01 (2003) 035.
[10] A. de Gouvea and H. Murayama, Statistical test of anarchy, Phys. Lett. B **573**, 94 (2003).
[11] J. R. Espinosa, Anarchy in the neutrino sector?, arXiv:hep-ph/0306019.
[12] A. de Gouvea and H. Murayama, Neutrino mixing anarchy: Alive and kicking, Phys. Lett. B **747**, 479 (2015).
[13] G. Altarelli, F. Feruglio, I. Masina, and L. Merlo, Repressing anarchy in neutrino mass textures, J. High Energy Phys. 11 (2012) 139.
[14] V. Brdar, M. Konig, and J. Kopp, Neutrino anarchy and renormalization group evolution, Phys. Rev. D **93**, 093010 (2016).
[15] M. L. Mehta, *Random Matrices* (Academic Press, New York, 2004), Vol. 142.
[16] Y. Bai and G. Torroba, Large $N(=3)$ neutrinos and random matrix theory, J. High Energy Phys. 12 (2012) 026.
[17] J. Bergstrom, D. Meloni, and L. Merlo, Bayesian comparison of U(1) lepton flavor models, Phys. Rev. D **89**, 093021 (2014).
[18] X. Lu and H. Murayama, Neutrino mass anarchy and the Universe, J. High Energy Phys. 08 (2014) 101.
[19] K. S. Babu and S. M. Barr, Large neutrino mixing angles in unified theories, Phys. Lett. B **381**, 202 (1996).
[20] M. J. Strassler, Generating a fermion mass hierarchy in a composite supersymmetric standard model, Phys. Lett. B **376**, 119 (1996).
[21] A. E. Nelson and M. J. Strassler, Realistic supersymmetric model with composite quarks, Phys. Rev. D **56**, 4226 (1997).
[22] C. D. Froggatt and H. B. Nielsen, Hierarchy of quark masses, Cabibbo angles and *CP* violation, Nucl. Phys. **B147**, 277 (1979).
[23] K. S. Babu, T. Enkhbat, and I. Gogoladze, Anomalous U(1) symmetry and lepton flavor violation, Nucl. Phys. **B678**, 233 (2004).
[24] K. S. Babu and T. Enkhbat, Fermion mass hierarchy and electric dipole moments, Nucl. Phys. **B708**, 511 (2005).
[25] K. Agashe, T. Okui, and R. Sundrum, A Common Origin for Neutrino Anarchy and Charged Hierarchies, Phys. Rev. Lett. **102**, 101801 (2009).
[26] F. Feruglio, K. M. Patel, and D. Vicino, Order and anarchy hand in hand in 5D SO(10), J. High Energy Phys. 09 (2014) 095.
[27] F. Brummer, S. Fichet, and S. Kraml, The supersymmetric flavour problem in 5D GUTs and its consequences for LHC phenomenology, J. High Energy Phys. 12 (2011) 061.
[28] K. Yoshioka, On fermion mass hierarchy with extra dimensions, Mod. Phys. Lett. A **15**, 29 (2000).
[29] P. Minkowski, $\mu \to e\gamma$ at a rate of one out of 10^9 muon decays?, Phys. Lett. **67B**, 421 (1977); T. Yanagida, in *Proceedings of the Workshop on Unified Theories and Baryon Number in the Universe* (KEK, Tsukuba, 1979), edited by A. Sawada and A. Sugamoto; S. Glashow, in *Cargese 1979, Proceedings, Quarks and Leptons* (Springer, New York, 1979); M. Gell-Mann, P. Ramond, and R. Slansky, in *Supergravity: Proceedings of the Supergravity Workshop at Stony Brook* (North-Holland, Amsterdam, 1979), edited by P. Van Niewenhuizen and D. Freeman; R. Mohapatra and G. Senjanović, Neutrino Mass and Spontaneous Parity Violation, Phys. Rev. Lett. **44**, 912 (1980).
[30] C. H. Albright, K. S. Babu, and S. M. Barr, A Minimality Condition and Atmospheric Neutrino Oscillations, Phys. Rev. Lett. **81**, 1167 (1998).
[31] J. Sato and T. Yanagida, Large lepton mixing in a coset space family unification on $E(7)/SU(5) \times U(1)^3$, Phys. Lett. B **430**, 127 (1998).
[32] N. Irges, S. Lavignac, and P. Ramond, Predictions from an anomalous U(1) model of Yukawa hierarchies, Phys. Rev. D **58**, 035003 (1998).
[33] N. Maekawa, Neutrino masses, anomalous U(1) gauge symmetry and doublet-triplet splitting, Prog. Theor. Phys. **106**, 401 (2001).
[34] H. Georgi and C. Jarlskog, A new lepton-quark mass relation in a unified theory, Phys. Lett. **86B**, 297 (1979).
[35] See for, e.g., I. Dorsner and P. Fileviez Perez, Unification versus proton decay in SU(5), Phys. Lett. B **642**, 248 (2006).
[36] N. Haba, Composite model with neutrino large mixing, Phys. Rev. D **59**, 035011 (1999).
[37] S. M. Barr and H. Y. Chen, A simple grand unified relation between neutrino mixing and quark mixing, J. High Energy Phys. 11 (2012) 092.
[38] S. M. Barr and H. Y. Chen, Model of quark and lepton mixing and mass hierarchy, Phys. Rev. D **93**, 053009 (2016).
[39] S. Antusch and V. Maurer, Running quark and lepton parameters at various scales, J. High Energy Phys. 11 (2013) 115.
[40] Z. z. Xing, H. Zhang, and S. Zhou, Updated values of running quark and lepton masses, Phys. Rev. D **77**, 113016 (2008).
[41] K. S. Babu, Renormalization group analysis of the Kobayashi-Maskawa matrix, Z. Phys. C **35**, 69 (1987).
[42] V. D. Barger, M. S. Berger, and P. Ohmann, Universal evolution of CKM matrix elements, Phys. Rev. D **47**, 2038 (1993).
[43] J. F. Donoghue, K. Dutta, and A. Ross, Quark and lepton masses and mixing in the landscape, Phys. Rev. D **73**, 113002 (2006).
[44] G. L. Fogli, E. Lisi, A. Marrone, D. Montanino, A. Palazzo, and A. M. Rotunno, Global analysis of neutrino masses, mixings and phases: Entering the era of leptonic *CP* violation searches, Phys. Rev. D **86**, 013012 (2012).
[45] V. D. Barger, M. S. Berger, and P. Ohmann, Supersymmetric grand unified theories: Two loop evolution of gauge and Yukawa couplings, Phys. Rev. D **47**, 1093 (1993).